AMERICAN UNIVERSITY OF BEIRUT

MICRORNA-126-3P: POTENTIAL PLAYER IN BREAST CANCER TUMORIGENESIS

by
ZAHRAA SHEHAB MSHEIK

A thesis
submitted in partial fulfillment of the requirements
for the degree of Master of Biomedical Sciences
to the Department of Anatomy, Cell Biology, and Physiological Sciences
of the Faculty of Medicine
at the American University of Beirut

Beirut, Lebanon
September 2020

AMERICAN UNIVERSITY OF BEIRUT

MICRORNA-126-3P: POTENTIAL PLAYER IN BREAST CANCER TUMORIGENESIS

BY

ZAHRAA SHEHAB MSHEIK

Approved by:

Dr. Rihab Nasr, Associate Professor
Department of Anatomy, Cell Biology,
and Physiological Sciences
Advisor

Dr. Georges Daoud, Associate Professor
Department of Anatomy, Cell Biology,
and Physiological Sciences
Member of Committee

Dr. Samia Khoury, Associate Dean and Professor
Department of Neurology
Member of Committee

Dr. Raya Saab, Associate Professor
Department of Pediatrics and Adolescent Medicine
Member of Committee

Date of thesis defense: September 8, 2020

AMERICAN UNIVERSITY OF BEIRUT

THESIS, DISSERTATION, PROJECT RELEASE FORM

Student Name: MsheiK Zahraa Shehab
Last First Middle

● Master's Thesis ○ Master's Project ○ Doctoral Dissertation

☐ I authorize the American University of Beirut to: (a) reproduce hard or electronic copies of my thesis, dissertation, or project; (b) include such copies in the archives and digital repositories of the University; and (c) make freely available such copies to third parties for research or educational purposes.

■ I authorize the American University of Beirut, to: (a) reproduce hard or electronic copies of it; (b) include such copies in the archives and digital repositories of the University; and (c) make freely available such copies to third parties for research or educational purposes after:

One ---- year from the date of submission of my thesis, dissertation, or project.
Two ---- years from the date of submission of my thesis, dissertation, or project.
Three ---- years from the date of submission of my thesis, dissertation, or project.

Zahraa 18/9/20

Signature Date

ACKNOWLEDGMENTS

First, I am thankful and grateful to God, the most gracious, the most merciful, for giving me the strength to complete this work.

I would like to express my sincere gratitude to my advisor Doctor Rihab Nasr, a powerful woman and role model I seek to be in the future. I am so thankful for providing me with continuous personal and professional guidance, support, and encouragement throughout my whole journey. I highly appreciate all your time contribution to make my experience productive and stimulating.

I would like to thank my committee members Doctor Georges Daoud, Doctor Raya Saab, and Doctor Samia Khoury for their time to review my manuscript and give me insightful comments.

My sincere thanks and gratitude to Ms. Ghada Chamandi and Dr. Farah Nassar for devoting so much time in mentoring and guiding me throughout this entire process. I am so grateful for the support and trust that you've shown me. Thank you, Ghada, for dedicating a lot of your time to teach me technical work and help me troubleshoot. Thank you for your patience, for all the fun times that we had together, and for being there in every ups and downs. Thank you, Farah, for guiding me on how to be a good researcher, how to troubleshoot, and for all our personal and scientific discussions. I owe gratitude to both of you.

I thank my fellow lab mates, Amro, Wafaa, and Maha, for being a great team to work with and for all the fun times we had together. A special thanks to my friend and colleague Nour Maatouk for being a great support and for always having time to listen to me. I would like to thank the core facility members especially, Maria Esmerian, and neighboring lab members who were always ready to help. I would also like to thank the Medical Practice Plan for funding the project.

Finally, I am so thankful and grateful to my family members, especially my sisters, Hiba and Zeinab, for all the sacrifices that they've made on my behalf. I owe all my success to you. No words can describe how grateful I am for your support that shapes who I am today and will be in the future.

AN ABSTRACT OF THE THESIS OF

Zahraa Shehab Msheik for Master of Biomedical Sciences
Major: Physiology

Title: microRNA-126-3p: Potential Player in Breast Cancer Tumorigenesis

Background: Breast cancer (BC) is a major health burden that affects over one million women each year. It is the most prevalent cancer in women and number one cancer killer of them worldwide. BC is a heterogenous type of cancer composed of different subtypes characterized by distinct clinical outcomes. Thus, uncovering new players in breast cancer development might lead to better understanding of its tumorigenesis. During the past two decades, research has shed lights on microRNAs (miRNAs) as potential players in the development of several diseases including cancer. These small, noncoding RNA molecules are aberrantly expressed in breast cancer and play diverse roles in its tumorigenesis. Recently, our group has shown a panel of miRNA dysregulated in Lebanese BC tissues by conducting microarray profiling analysis. Of these miRNAs, miR-126-3p was significantly downregulated. Thus, our aim was to determine the role of miR-126-3p in BC progression.

Methods and Results: Downregulation of miR-126 in Lebanese BC tissues was validated using RT-qPCR. miR-126 levels were modulated in BC cell lines (MCF-7 and MDA-MB-231) and non-tumorigenic cell line (MCF-10A) by transfection with miR-126 mimic. MTT assay, PI analysis, and colony formation assay were done to determine the effect of overexpressing miR-126 on these cell lines. miR-126 had no effect on MCF-10A and MDA-MB-231 cell proliferation but, significantly decreased MCF-7 proliferation. No effect was detected on cell cycle progression whereas a trend towards a decrease was detected in the number of mammospheres upon transfection with miR-126 mimic. Then, *in silico* analysis was done to determine the potential targets of the corresponding miRNA. PLXNB2, SLC7A5, SPRED1, PLK2, HOXA9, MMP7, CRK, and IRS1 were selected as potential targets of miR-126. RT-qPCR data showed that miR-126 overexpression significantly downregulated SLC7A5 and PLXNB2 mRNA levels. Finally, *in silico* KM analysis was done to determine the correlation between miR-126 or SLC7A5 expression and overall survival (OS) of BC patients. Importantly, high expression of miR-126 or low expression of SLC7A5 correlated with better OS of ER+ patients.

Conclusion: Overall, our study suggests that miR-126 might play a tumor suppressor role in breast cancer through the modulation of different mRNA targets. However, further studies are required to validate its role. miR-126 might also be considered a potential prognostic biomarker in breast cancer.

CONTENTS

ILLUSTRATIONS

TABLES

ABBREVIATIONS

ADAM9	A Disintegrin and Metalloproteinase 9 Domain
AGO	Argonaute
AJCC	American Joint Committee on Cancer
AR	Androgen Receptor
ASR	Age-Standardized Rate
BC	Breast Cancer
BRCA	Breast Cancer Gene
CA153	Cancer Antigen 153
CDK	Cyclin-dependent Kinase
CEA	Carcinoembryonic Antigen
CRK	CRK proto-oncogene, adaptor protein
CSCs	Cancer Stem Cells
CTL	Untransfected or Control
DCIS	Ductal Carcinoma in situ
DGCR8	DiGeorge Syndrome Critical Region 8
DMEM	Dulbecco's Modified Eagle's Medium
EBC	Early Breast Cancer
EGF	Epidermal Growth Factor
EGFL-7	Epidermal Growth Factor-Like Domain 7
EGFR	Epidermal Growth Factor Receptor
EMT	Epithelial-Mesenchymal Transition
ER/ ER-β	Estrogen Receptor/ Estrogen Receptor Beta
FBS	Fetal Bovine Serum
FC	Fold Change
FFPE	Formalin-Fixed Paraffin Embedded
GAPDH	Glyceraldehyde 3-phosphate dehydrogenase
HBSS	Hank's Balanced Salt Solution
HER2	Human Epidermal Growth Factor Receptor 2
HOXA9	Homeobox A9
IDC	Invasive Ductal Carcinoma
ILC	Invasive Lobular Carcinoma
IRS1	Insulin Receptor Substrate 1
KM	Kaplan-Meier
LCIS	Lobular Carcinoma in situ
miRISC	miRNA-Induced Silencing Complex

miRNA/miR	microRNA
MMP7	Metalloprotease 7
MRI	Magnetic Resonance Imaging
mRNA	messenger RNA
mTOR	Mammalian Target of Rapamycin
MTT	3-(4,5-Dimethylthiazol-2-Yl)-2,5-
NAT	Normal Adjacent Tissue
NC	Negative Control
NRT	No Reverse Transcription Control
NTC	No Template Control
oncomiRs	Oncogenic microRNAs
OS	Overall Survival
PARP	Poly-ADP-Ribose-Polymerase
PBS	Phosphate Buffered Saline
PI	Propidium Iodide
PI3K	Phosphatidylinositol-3-kinase
PLK2	Polo-Like Kinase 2
PLXNB2	Plexin B2
PR	Progesterone Receptor
Pre-miRNAs	Precursor microRNAs
Pri-miRNAs	Primary microRNAs
RGS3	Regulator of G-protein Signaling 3
RT-qPCR	Real-Time Quantitative Polymerase Chain Reaction
SEM	Standard Error of Mean
shRNA	Short-Hairpin RNA
SLC7A5	Solute Carrier Family 7 Member 5
SPRED1	Sprouty-Related EVH1 Domain Containing 1
TDLU	Terminal-Ductal Lobular Unit
TN	Triple Negative
TNBC	Triple Negative Breast Cancer
TNM	Tumor Node Metastasis
TP	Triple Positive
TRBP	Transactivation-responsive RNA-Binding Protein
TRI	Trizol
tsmiRs	Tumor Suppressor microRNAs
US	Ultrasonography
UTR	Untranslated Region
VEGF	Vascular Endothelial Growth Factor
XPO5	Exportin 5

CHAPTER I

INTRODUCTION

A. Breast Cancer

1. Epidemiology and Risk Factors

a. Worldwide

Breast cancer (BC) is the most frequent cancer and the leading cause of cancer death in women worldwide. In 2018, it was estimated that BC in women accounts for 24.2% of all cancer cases and 15% of all cancer mortalities [1] (Figure 1A). BC incidence and mortality rates vary considerably between different regions of the world. While the age-standardized rate (ASR) of BC incidence in developed countries is higher than that in developing ones (54.4 per 100,000 versus 31.3 per 100,000, respectively), the relative mortality rate is higher in developing countries (14.9 per 100,000 versus 11.6 per 100,000, respectively) [1]. The overall incidence of BC in Asia is lower, though increasing, compared to the average world level and some developed regions such as Europe and America. However, this incidence varies within different regions of Asia with ASR of incidence that ranges between 45.3 per 100,000 in Western Asia and 25.9 per 100,000 in South-Central Asia [1, 2]. Notably, increase in BC incidence is mainly due to the adoption of "Westernized" lifestyle and diet, including late childbearing, having fewer children, and consumption of calorie-dense food [3].

a. Lebanon

Similar to the global status, BC in Lebanon is the most common and major cause of cancer mortality among women. According to GLOBOCAN 2018, BC in Lebanon accounts for 37.9% of all cancer cases and 23.1% of all cancer deaths (Figure 1B). A recent estimation of ASR of incidence in Lebanon is 96.5 per 100,000, which is the highest compared to other regional countries such as Kuwait (56.1 per 100,000) and Saudi Arabia (24.5 per 100,000) [4]. This variation in the reported BC incidence rates between the different Arab countries could be partly explained by the disparity in the implementation of screening programs, awareness campaigns, and proper registries. Reduced awareness campaigns and screening programs in regional countries like Saudi Arabia have led to the prevalence of advanced BC cases, but lower reported incidence rates [4, 5]. Moreover, the increase in BC incidence in Lebanon is attributed to other factors, including reproductive factors such as the increase in the mean marital age and menopause, decreased fertility rate and age at menarche, and use of hormonal replacement therapy. Other protective factors like breastfeeding and the traditional Mediterranean diet are thought to be less prevalent within the current Lebanese population [4, 5]. In addition, obesity has been shown to be associated with a higher incidence of BC in postmenopausal women [6]. Active and passive smoking are also a possible risk factor of BC, especially that Nargileh smoking is rising fast throughout the Lebanese population [7].

The median age of BC diagnosis in Lebanon is 50 years, which is less than that of Western countries (63 years) [8]. A high percentage of Lebanese BC patients are younger than 40 years old, constituting 18-20% of all BC cases in Lebanon. This high percentage is

in sharp contrast with the West, where only 6.6% of Western BC patients are younger than 40 years [9]. A study conducted on 1,320 Lebanese BC patients had shown that breast cancer in young women foreshadows a worse prognosis. A high percentage of young patients developed metastasis and had worse survival despite hormonal therapy; in addition, they were characterized by a higher tumor grade than their older counterparts [10]. This particularity in the Lebanese population was not associated with the *BRCA* mutations. A study conducted on 250 Lebanese young BC patients has shown that only 5.6% carried deleterious mutations in the homologous recombinant genes *BRCA1* and *BRCA2* [11]. In a more recent study conducted on 281 Lebanese breast/ovarian cancer patients, with a mean age of BC patients of 47.7 years, 7.8% had *BRCA1/2* gene mutations with the prevalence of c.131G > T mutation in *BRCA1* [12]. This particular mutation could be considered as a founder mutation in the Lebanese population since it has been detected in different studies [11, 12]. However, this percentage is still lower than expected when compared to studies from industrialized regions. Thus, *BRCA* mutations are not the leading cause behind the observed high percentage of BC in young Lebanese women. So, it is crucial to look for alternative gene mutations and other factors that might contribute to the development of early BC.

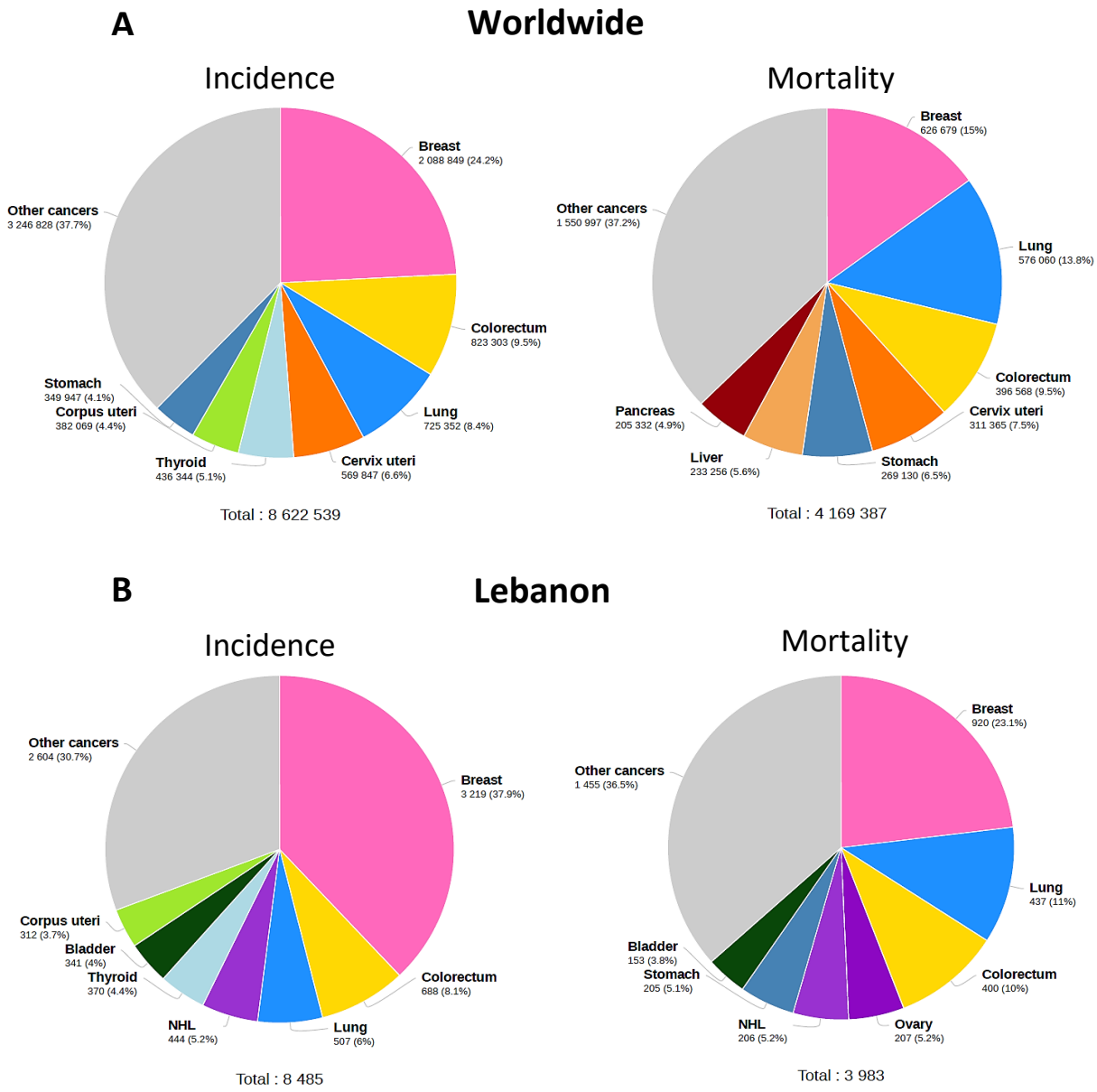

Figure 1. Breast Cancer Incidence and Mortality among Women in the World (A) and in Lebanon (B) (GLOBOCAN, 2018). Breast cancer has the highest incidence and mortality among females in the World and Lebanon.

2. Mammary Gland Development and Anatomy

The female breast is located on the anterior thoracic wall with its base extending from the second to the sixth rib [13]. A thorough understanding of normal breast development and anatomy is indispensable to understand BC development.

The human breast houses the mammary glands, a modified type of apocrine glands that are specialized to produce and deliver milk through an extensive network of branched ducts [13, 14]. The breast tissue is composed of parenchyma and stroma originating from the ectodermal and mesodermal elements, respectively. The parenchyma consists of the branched ductal system and secretory alveoli, whereas the stroma consists of the adipose tissue, blood vessels, fibroblasts, and leukocytes that provide the environment for the parenchyma development [14, 15]. The breast is composed of 15 to 20 lobes which are divided further into 20 to 40 lobules that consist of the branched ductal glands. Each lobe drains into a major lactiferous duct that dilates into a lactiferous sinus, which eventually opens onto the nipple. The space between the different lobes is occupied by the adipose tissue (Figure 2A) [13].

Development of mammary glands involves three main stages: embryonic, pubertal, and reproductive [15, 16]. Mammary glands start to develop at the fifth week of fetal life from two thickened ectoderm bands, the mammary crests. In humans, the mammary crests deteriorate as the embryo develops except for paired epithelial masses in the pectoral region that give rise to the primary mammary buds. These are ingrowth of the ectoderm into the underlying mesenchyme. The primary buds then develop 15-20 secondary buds that will eventually form the lactiferous ducts and their branches. Major

lactiferous ducts develop and open into a mammary pit that transforms into a nipple during infancy (Figure 2B-G).

At birth, the mammary glands remain rudimentary, consisting of only the main lactiferous ducts until puberty [13, 14]. Prenatal human breast development does not differ between males and females. Sexually dimorphic development begins at puberty, which is highly regulated by sex hormones [14]. At puberty, massive proliferation occurs leading to the formation of a branched ductal network in a process known as branching morphogenesis. This process is under the influence of the ovarian hormones' estrogen and progesterone, and the pituitary growth factors. Lateral branches give rise to the terminal ducts that will eventually form the functional unit of the breast known as the terminal-ductal lobular units (TDLUs) comprising of numerous blind-ended ductules called acini. This tree-like pattern of ducts occupies most of the breast space; the remainder of the space is occupied by the adipose tissue, blood vessels, immune cells, and fibroblasts [14, 16]. The reproductive changes include those that occur during pregnancy, lactation, and involution. Upon pregnancy, the mammary glands undergo maturation and alveologenesis under the influence of progesterone and prolactin. The first transformation of pregnancy is a tremendous increase in the ductal network, providing ductal arbors for the second transformation, which is the alveoli development that will become the milk-secreting cells during lactation. The final ductal network consists of an outer basal myoepithelial cell layer and an inner luminal cell layer, where the latter is composed of ductal luminal cells that line the inside of the ducts and alveolar luminal cells that secrete milk during lactation [14, 16]. After delivery, prolactin, along with growth hormones, induces milk production and

secretion by the alveolar luminal epithelial cells, which is facilitated by the contraction of the myoepithelial cells [13, 16]. Upon weaning, the lack of milk demand initiates involution that is characterized by the apoptosis of the alveolar cells, the collapse of the alveoli, and remodeling of the epithelial tree into a simple ductal one [13, 16].

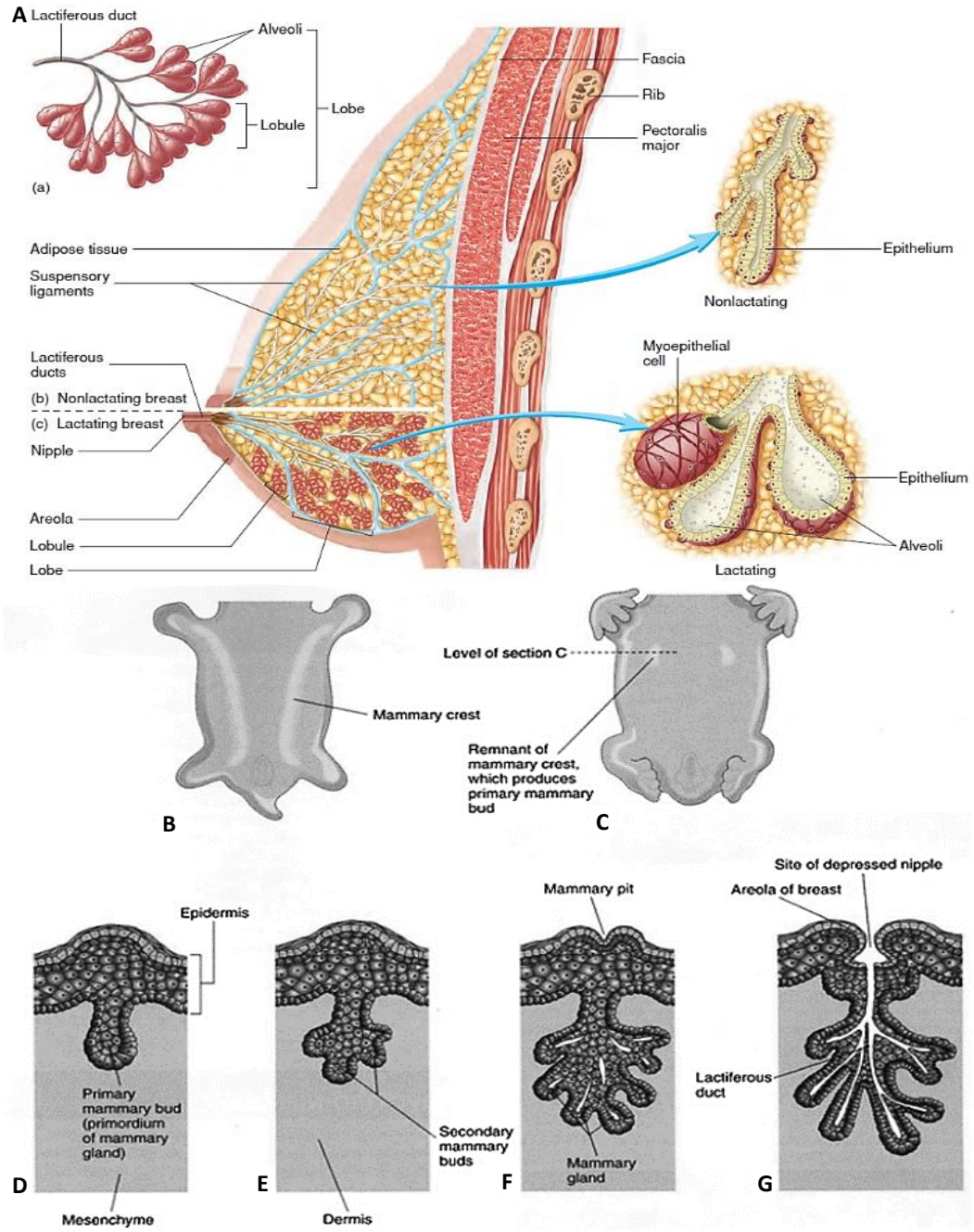

Figure 2. Mammary Gland Development and Anatomy. (A): Representation of the breast anatomy showing the differences between lactating and nonlactating breasts. Adopted from Essentials of Anatomy and Physiology, BrainKart.com. (B): Ventral view of an embryo showing the mammary crests. (C): Similar view showing the remains of the mammary crests. (D-G): Transverse sections showing the successive stages of the mammary gland development. Adopted from Javed, A. and A. Lteif, Development of the human breast. Semin Plast Surg, 2013.

3. Breast Cancer Origin and Evolution

The human breast is characterized by cellular plasticity with extensive remodeling in adulthood, which increases its susceptibility to carcinogenesis [14]. Like any other type of cancer, BC is driven by genetic and epigenetic alterations that affect key processes involved in cell growth and development [17]. These changes were described primarily in the epithelial cells; however, several studies have shown that the microenvironment also plays a role in BC initiation and progression [18-20]. Normally, breast ducts consist of a single layer of luminal epithelial and myoepithelial cells lined by a basement membrane. BC develops first through ductal hyperproliferation, where the luminal epithelial cells grow abnormally. Then, the tumor evolves into in situ carcinoma where the cancerous cells are within the ducts or the lobules. Subsequently, the basement membrane is degraded, and tumor cells can invade the surrounding tissues and migrate to distant organs, including the brain, lungs, liver, and bones, eventually leading to metastasis and resulting in the progression of the tumor to invasive carcinoma. This progression might be mediated by the abnormal myoepithelial cells and the surrounding stromal cells. Family history is one of the determinants of BC development. It includes hereditary mutations, mainly in *BRCA1* and *BRCA2* genes, in addition to mutations in other genes such as *TP53* and *TGFB1* [21, 22].

4. Breast Cancer Classifications

BC is not a single disease, rather, it is a heterogeneous one composed of different subtypes characterized by distinct clinical outcomes and response to treatments [21]. It is characterized by intertumor heterogeneity that differs among patients and intratumor

heterogeneity that differs within each individual tumor [23]. Understanding this heterogeneity is essential for the development of targeted therapies. BC is classified according to histopathology, immunopathology, mRNA expression profiling (molecular), and microRNA expression signatures (Figure 3) [24].

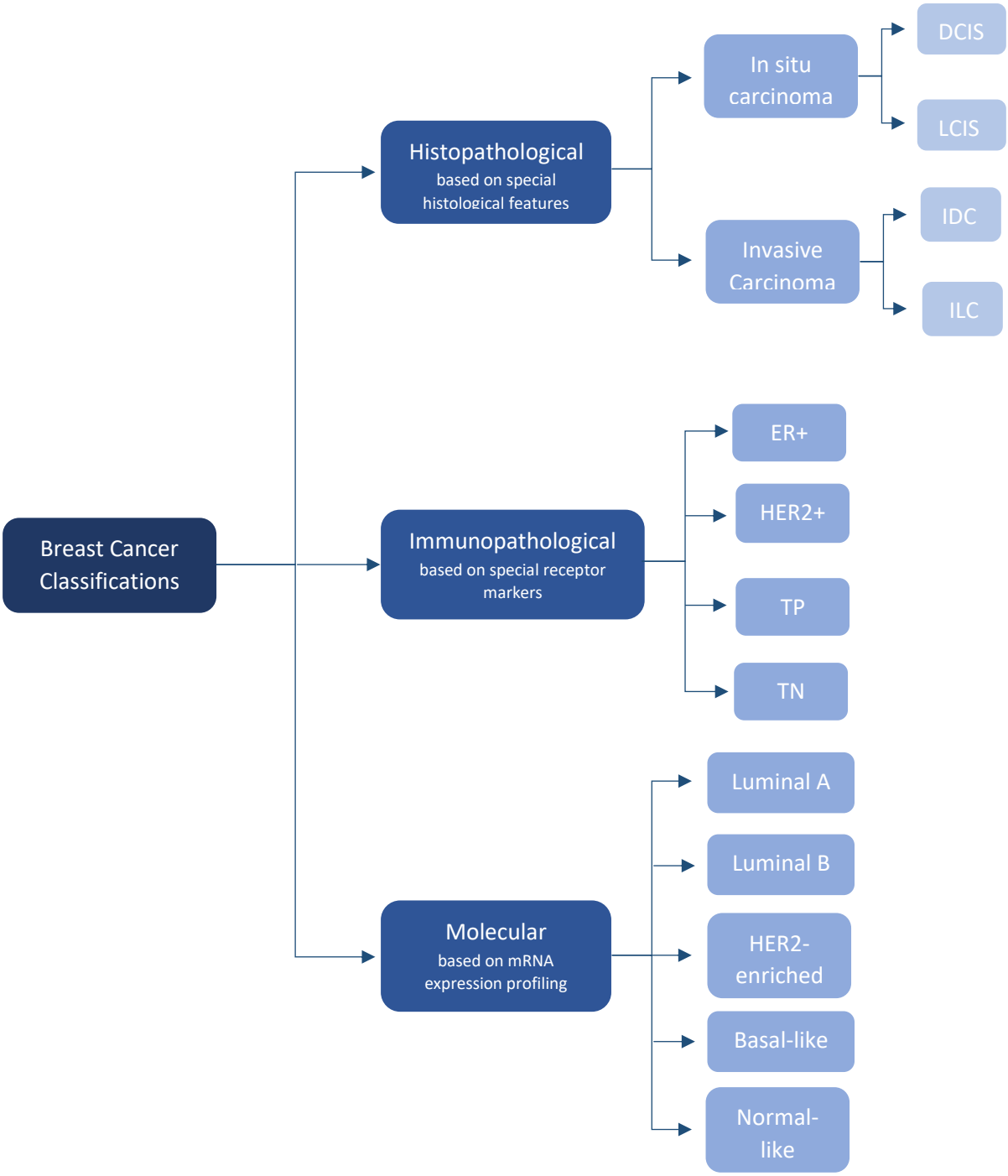

Figure 3. Summary of the Intertumor Heterogeneity of Breast Cancer. Breast cancer is classified by its histopathological features, immunopathological features, mRNA expression profiling (molecular), and miRNA expression signatures. DCIS: ductal carcinoma in situ, LCIS: lobular carcinoma in situ, IDC: invasive ductal carcinoma, ILC: invasive lobular carcinoma, ER+: estrogen receptor positive, HER2+: human epidermal growth factor receptor 2 positive, TP: triple positive, TN: triple negative.

Histopathologically, BC is classified by its histological appearance into in situ and invasive (infiltrating) carcinomas, which are further subclassified into ductal or lobular. This subclassification was previously based on the site from which the tumor originated; ductal carcinomas are tumors originating from the ducts whereas lobular carcinomas are tumors originating from the lobules. However, it is now found that this sort of classification is not related to the origin of tumor development, since both are found to originate from the TDLUs, rather, it is related to the expression of the cell-cell adhesion molecule E-cadherin [25, 26]. Still, the terms “ductal” and “lobular” have persisted. E-cadherin is a member of the calcium-dependent cell adhesion molecules (CAMs) that plays an important role in cell-cell adhesion in epithelial cells. E-cadherin is a tumor suppressor gene, and loss of its function results in increased invasiveness and metastasis of tumors [27]. Ductal carcinoma in situ (DCIS) is considered a non-obligatory precursor lesion for the subsequent development of invasive breast cancer. Lobular carcinoma in situ (LCIS) is less common than DCIS and distinguished by the lack of E-cadherin expression. DCIS and LCIS are further subclassified into distinct histological variants based on different cytoarchitectural features [25]. Invasive ductal carcinoma (IDC) is a malignant ductal proliferation characterized by stromal invasion [25]. It is the most common histological subtype of invasive breast carcinoma contributing to 40-75% of them all [23]. With time, IDC can spread via the lymph nodes to other parts of the body [17, 26]. Invasive lobular carcinoma (ILC) is the second most common invasive breast carcinoma accounting for 5-15% of the cases [25]. It occurs in the terminal lobules of the breast and can invade the surrounding breast tissue, but it is still less aggressive than IDC [26]. Other less common

histopathological subtypes include medullary, mucinous (colloid), and papillary carcinomas, in addition to several others [17].

Immunopathologically, BC is classified based on the presence of specific receptor markers that not only define the different subtypes but also, define their response to targeted therapy. These chief markers are the estrogen receptor (ER), the progesterone receptor (PR), and the human epidermal growth factor receptor 2 (HER2 or ERBB2) that are assessed by immunohistochemistry (IHC)-based methods [24, 28]. A combination of these markers subdivides BC into different categories, including ER+ (ER+, HER2-), HER2+ (ER-, HER2+), triple positive (ER+, PR+, HER2+), and triple negative (ER-, PR-, HER2-) [24]. Estrogen and progesterone receptor positive tumors constitute 80% and 60-70% of all breast carcinomas, respectively [29, 30]. ER+ tumors respond better to endocrine therapy, which includes ER antagonists, mainly tamoxifen (block ER signal transduction pathways), and aromatase inhibitors (block estrogen synthesis) [31, 32]. Multiple studies have shown that ER+/PR- tumors are less responsive to endocrine therapies than the ER+/PR+ ones [29, 33, 34]. 15-20% of breast carcinoma overexpress HER2, a membrane tyrosine kinase oncoprotein [35]. HER2+ cases are targeted with monoclonal antibodies, mainly trastuzumab, that disrupts HER2-dependant signaling pathways [36]. As for triple negative breast cancer (TNBC), which is defined by the lack of expression of the three receptors, it contributes to 10-15% of all breast cancers [37]. It is characterized by being the most aggressive subtype of BC with high recurrence, metastatic, and mortality rates. Treatment options of TNBC are limited to the cytotoxic chemotherapy since the endocrine therapy and HER2-targeted therapy are not effective [38]. However,

several recent studies have shown that targeting PARP, poly-adenosine diphosphate ribose polymerase that regulates the DNA base-excision repair pathway, along with chemotherapy, serves as a potential targeted therapy for TNBC harboring mutations in the *BRCA* genes [39, 40]. From a prognostic point of view (Figure 4), the best overall prognosis is for ER+ (ER+, HER2-) tumors followed by HER2+ (ER-, HER2+) and triple positive (ER+, PR+, HER2+) when treated with HER2-targeted therapies, and the worst prognosis is for the TN (ER-, PR-, HER2-) tumors [41, 42]. Other potential immunohistochemical markers have been proposed for use in BC management. These include ER-β (estrogen receptor beta), androgen receptor (AR), and Ki-67 [28]. Ki-67 is a nuclear protein involved in cell proliferation. It has been shown that Ki-67 positivity correlates with overall shorter survival of BC patients [43].

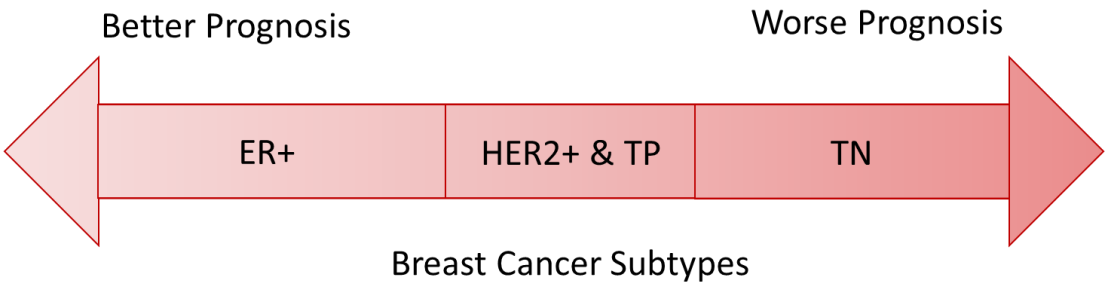

Figure 4. Prognosis of the Immunopathological Breast Cancer Subtypes. ER+ (ER+, HER2-): best prognosis, HER2+ (ER-, HER2+) and triple positive (ER+, PR+, HER2+): better prognosis, triple negative (ER-, PR-, HER2-): worst prognosis.

Molecularly, Perou et al. classified BC into different subtypes based on their gene expression pattern (Table 1). This classification, which was later updated, provided better predictions of the different subtypes responses to therapies [44]. It includes [45-47]:

a. Luminal A: ER+/PR+ and HER2-, characterized by good prognosis, low histological grade, and low proliferation (Ki-67<14%). Since it is ER+, Luminal A tumors respond best to endocrine therapy.
b. Luminal B: ER+ and/or PR+, HER2+ or HER2-, characterized by poorer prognosis, higher histological grades, and higher proliferation (Ki-67≥14%) compared to Luminal A. This subtype is also sensitive to endocrine therapy but to a lesser extent than Luminal A.
c. HER2-enriched: ER-/PR- and HER2+, characterized by poor prognosis and high grade. This tumor is responsive to HER2-monoclonal targeted therapy.
d. Basal-like: ER-/PR- and HER2-, resembles TNBC, highly aggressive, characterized by high tumor grade and the worst prognosis. It has no response to endocrine therapy but appears to be sensitive to PARP inhibitors.
e. Normal-like: resembles the normal tissue where it expresses genes shared with the normal epithelial cells and is associated with good prognosis.
f. More recently, a new subtype, claudin-low, has been identified to display gene expression patterns similar to the mammary stem cells [48].

A new area for understanding BC behavior has arisen with the discovery of microRNA that can further classify BC into different subtypes [49]. This will be further described below.

Table 1. Summary of the Immunohistochemical Profile and Prognosis of the Molecular Breast Cancer Subtypes.

Molecular Classification				
	Luminal A	**Luminal B**	**HER2 enriched**	**Basal-like**
ER, PR	ER+ PR+	ER+ and/or PR+	ER- PR-	ER- PR-
HER2, others	HER2- Low Ki-67 (<14%)	HER2+ or HER2- High Ki-67 (≥14%)	HER2+	HER2- CK5/6+ and/or EGFR+
Prognosis	Good	Poorer	Poor	Poorest

5. Breast Cancer Staging System

The tumor-node-metastasis (TNM) staging system was developed by the American Joint Committee on Cancer (AJCC), where it stages cancer based on the major morphological features of the tumor that are thought to influence prognosis (Table 2). Staging of BC is based on the primary tumor size (T), regional lymph node involvement (N), and distant metastasis status (M). Nine stages (0, IA, IB, IIA, IIB, IIIA, IIIB, IIIC, IV) have been designed based on different combinations of T, N, and M status. Primary tumor size ranging from ≤20mm to >50mm are denoted as T1 to T3, T0 denoted for no measurable primary tumor, and T4 for tumor of any size with direct extension to chest wall and/or skin. Regional lymph node metastasis includes metastasis to the ipsilateral axillary, supraclavicular, and internal mammary lymph nodes. These are denoted as N0 for no involvement to N3 for extensive lymph node involvement. As for distant metastasis, it includes the contralateral lymph nodes, brain, lung, liver, and bone. These are designated as M0 for no metastasis and M1 for distant metastasis. In its latest edition, the committee incorporated the biomarkers (histologic grade, hormone receptor status, and HER2 status)

in addition to the multigene panel status into the traditional TNM staging system to create prognostic stages [50, 51]. Tumor grade is an important prognostic factor independent of the tumor size and lymph node involvement [52]. Worse prognosis is observed in tumors with a high histologic grade or poor differentiation compared to low histologic grade or well-differentiated tumors [53]. Hormone receptor status and HER2 status, along with Ki-67 expression, were also integrated into the system since ER and HER2 targeting agents have been shown to improve prognosis [31, 36]. Thus, the previously discussed molecular subtypes (luminal A, luminal B, HER2-enriched, and basal-like) were incorporated based on their respective prognosis. Among the multigene panel tests that measure the expression levels of a large panel of genes in BC, Oncotype DX showed the best evidence [54], thus, it is the one that was incorporated into the system. In addition, prognostic staging was adopted in the latest edition. Two prognostic groups were differentiated: clinical prognostic stage assigned to all patients regardless of the type of therapy given, and pathological prognostic stage assigned to patients who received surgery as initial treatment [50, 51].

Table 2. Summary of the Breast Cancer Staging System in the Eighth Edition of AJCC.

Traditional TNM Staging System	
T: Tumor Size	**T0:** no measurable tumor **T1:** tumor ≤20mm **T2:** tumor >20mm but ≤50mm **T3:** tumor >50mm **T4:** tumor of any size with direct extension to chest wall and/or to skin
N: Lymph Node Involvement	**N0:** no regional lymph node involvement **N1:** metastasis to ipsilateral axillary lymph nodes **N2:** metastasis to ipsilateral axillary or internal mammary lymph nodes **N3:** extensive lymph node involvement
M: Metastasis	**M0:** no distant metastasis **M1:** distant metastasis
New Additions to the Traditional Staging System	
Inclusion of Biomarkers: Tumor Grade, Hormone Receptor status, HER2 status	
Inclusion of Multigene Panels: Oncotype DX	
Adoption of Prognostic Staging: Clinical and Pathological Prognostic Stages	

6. Breast Cancer Diagnosis and Treatment

Several tests have been developed to detect BC. Mammography is considered the standard screening test for BC detection and diagnosis. However, it has some limitations such as low sensitivity in dense breasts, thus, it is less effective in and not recommended for young women [55, 56]. Other screening tests that might be utilized to detect malignant lesions in women with dense breasts include ultrasonography (US) and magnetic resonance imaging (MRI) but, each has its own limitations that compromise their potential as

screening tests for BC. US use is limited for the requirement of additional clinical experience and difficulty in interpretation criteria [57]. As for the MRI, although it is highly sensitive, it has low specificity and is expensive to be used routinely [58]. A definitive method to diagnose BC is a breast biopsy which is done as part of the triple test "clinical breast examination, breast imaging, and breast biopsy" to increase diagnostic accuracy [59]. Serum biomarkers such as the carcinoembryonic antigen (CEA) and cancer antigen 153 (CA153) are utilized as prognostic tools for BC, but they are not helpful in the early detection since they have low sensitivity and low specificity [60]. Other diagnostic and prognostic tests are the tissue-based multigene signature tests. These include: OncotypeDX, MammaPrint, Prosigna, EndoPredict, Breast Cancer Index, Mammostrat, and IHC4 that measure the expression levels of different genes in BC patients [61]. In addition, circulating microRNAs are differentially expressed in the serum of BC patients. Screening for microRNAs is feasible and may be considered as potential biomarkers useful for the detection of BC [62].

Treatments of BC usually include surgical excision, radio-, chemo-, hormonal, and targeted therapies. Surgical excision is done by removing either the part of the breast containing the tumor (lumpectomy) or the entire breast (mastectomy) [17]. As discussed previously, hormonal (endocrine) therapy is utilized for BC patients expressing estrogen and/or progesterone receptors, whereas targeted therapy is utilized for those expressing HER2. Both therapies have been shown to increase survival in BC patients [32, 36]. Other newly utilized targeted therapies include PARP inhibitors and those that target the PI3K/mTOR pathway and the cyclin-dependent kinases (CDKs) [63, 64].

B. microRNAs

microRNAs (miRNAs) are a class of small, endogenous, non-coding RNA molecules, approximately 22 nucleotides in length [65]. The first microRNA, *lin-4*, was discovered in 1993 by the Ambros group while studying the postembryonic developmental events in *Caenorhabditis elegans*. They have found that *lin-4* is not a protein-coding gene, instead, it encodes two small RNA transcripts that contain sequences complementary to the 3' untranslated region (3'-UTR) of *lin-14* mRNA, leading to a temporal decrease in LIN-14 protein. Therefore, they proposed that *lin-14* mRNA is post-transcriptionally regulated by *lin-4* miRNA [66]. Since then, several microRNAs have been discovered and some were shown to be highly conserved among different species, including humans, which raised the interest in the field of microRNA research [67, 68].

1. miRNA Biogenesis and Function

miRNA encoding genes are either intragenic, processed mostly from introns of protein encoding genes, or intergenic, transcribed independently and regulated by their own promoters [65]. Some miRNAs are transcribed polycistronically, as a single transcriptional unit, then processed into different miRNAs [69].

miRNAs are mainly transcribed by RNA polymerase II into long primary miRNAs (pri-miRNAs). The biogenesis of miRNAs can be done either through the canonical or the non-canonical pathway (Figure 5). The canonical pathway is the dominant one by which most of the miRNAs are processed. In this pathway, pri-miRNA is processed into a 70-nucleotide hairpin-shaped precursor miRNA (pre-miRNA) by the microprocessor

complex, which is composed of an RNA binding protein DiGeorge Syndrome Critical Region 8 (DGCR8) and a ribonuclease III enzyme Drosha. pre-miRNA is exported from the nucleus to the cytoplasm by an exportin-5 (XPO5)/Ran-GTP complex. It is then processed by the RNase III endonuclease Dicer and its cofactor transactivation-responsive RNA-binding protein (TRBP). This processing step involves the cleavage of the terminal loop, generating a mature miRNA duplex. The duplex is then loaded onto the Argonaute protein family (AGO 1-4 in humans) in an ATP-dependent manner. The strand with relatively unstable 5' end or that has a 5' U at nucleotide position 1 is selected as the guide "mature" miRNA strand that is retained in the AGO protein, whereas the "passenger" strand is cleaved by AGO2 or unwinds without cleavage [65, 70]. The non-canonical pathways can be grouped into Drosha/DGCR8-independent and Dicer-independent pathways. pri-miRNAs generated from introns by the Drosha/DGCR8-independent pathway are processed by a spliceosome machinery into pre-miRNAs which are exported by exportin-5, cleaved by Dicer, and loaded onto AGO protein [71]. These miRNAs are known as mirtrons. Another example of this pathway is the 7-methylguanosine (m^7G) capped pre-miRNAs (for example, miR-320) that are exported to the cytoplasm by exportin-1 then, cleaved by Dicer and loaded on AGO protein [72]. On the other hand, pre-miRNAs generated by the Dicer-independent pathway are processed by Drosha from endogenous short hairpin RNA (shRNA) molecules, then loaded onto AGO2 for further processing. Processing of miR-451 is an example of this pathway [73].

The guide strand, along with the AGO protein, is then incorporated into a large protein complex called miRNA-induced silencing complex (miRISC). Target specificity of

the miRISC complex is mediated by its interaction with complementary sequences on the target mRNAs. In animals, imperfect base-pairing occurs between the 5' seed region (nucleotides 2-8) of the miRNA and the 3'-UTR of the target mRNA. This interaction results in either repressing mRNA translation, decaying it by deadenylation and decapping, or degrading it by endonucleolytic cleavage [74-76]. However, other binding sites for miRNAs have been reported. These include the 5'-UTR, coding sequences, and promoter regions [77]. Binding to the promoter region has been shown to induce transcription, but more studies are needed to understand the functional significance of this interaction [78].

Thousands of miRNAs have been discovered and their roles in gene regulation have been well recognized. miRNAs are involved in multiple critical physiological as well as pathophysiological processes. Aberrant expression of miRNAs has been reported in a wide variety of human diseases such as diabetes, cardiovascular disorders, and cancer [79]. Still new miRNAs are being discovered and studied to determine their functions.

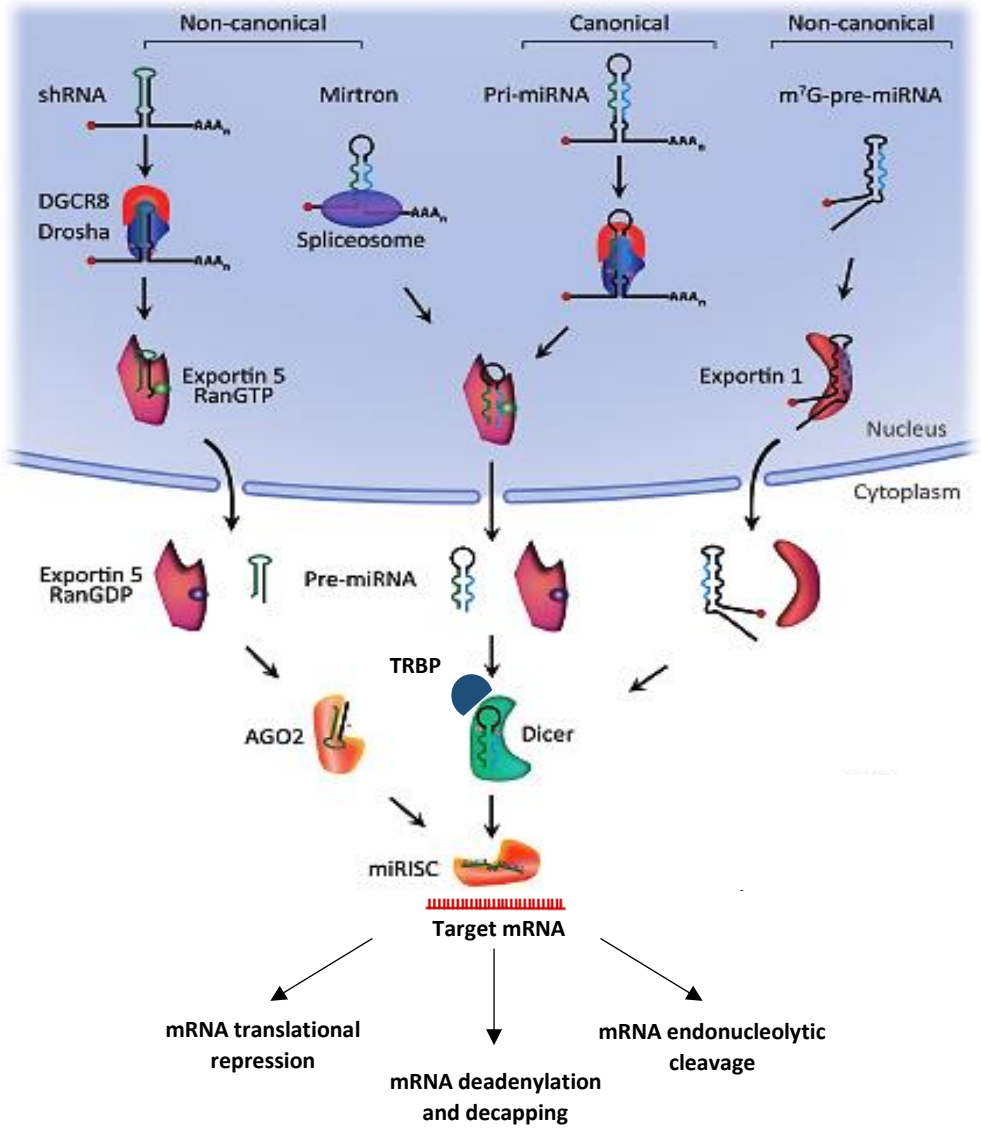

Figure 5. microRNA Biogenesis and Mode of Action. pri-miRNA generated by the canonical pathway is cleaved by the microprocessor complex DGCR8 and Drosha. The resulting pre-miRNA is exported to the cytoplasm by the exportin-5/Ran-GTP complex. pre-miRNA is further processed by Dicer and its cofactor TRBP generating a miRNA duplex that unwinds upon loading onto AGO protein. Mature miRNA strand incorporates into the miRISC complex and interacts with the target mRNA leading to its translational repression, deadynelation and decapping, or endonucleolytic cleavage. In the non-canonical pathways, miRNAs are either processed in a Drosha/DGCR8 independent (mirtrons and m^7G capped pre-miRNAs) or Dicer independent way. Modified from O'Brien et al., Overview of MicroRNA Biogenesis, Mechanisms of Action, and Circulation, 2018.

2. miRNAs in Biological Processes

miRNAs play different roles in several cellular and biological processes such as proliferation, apoptosis, angiogenesis, differentiation and development. miRNAs are reported to play distinct roles in the muscle and nervous system development. For instance, miR-124 and miR-128 are preferentially expressed in neurons whereas, miR-26 and miR-29 are more strongly expressed in astrocytes, indicating that miRNAs play a role in neuronal lineage differentiation [80]. Moreover, miRNAs play critical roles in immune system regulation. Dysregulation in the miRNA machinery may result in severe immune cell development defects and autoimmune diseases. For example, miR-181a was shown to play a role in T-cell selection and sensitivity to antigens [81].

3. miRNAs and Cancer

Dysregulation of miRNA expression profiles has been reported in numerous types of diseases including cancer. The first correlation between miRNA and cancer was reported in 2002 in chronic lymphocytic leukemia (CLL). miR-15 and miR-16 genes were shown to be frequently deleted or downregulated in the majority of CLL patients [82]. Since then, a great number of miRNAs were found to be dysregulated in a wide variety of cancers. For example, miR-21 was shown to be overexpressed in glioblastoma, breast, and colon cancer. On the other hand, miR-17-92 was found to be downregulated in hepatocellular carcinoma, retinoblastoma, and nasopharyngeal carcinomas [83]. miRNAs are classified as oncogenes (oncomiRs) or tumor suppressors (tsmiRs) based on their downstream targets. miRNAs are oncogenes if they downregulate tumor suppressors while they are tumor suppressors if they

downregulate oncogenes. miRNAs dysregulation in cancer could be attributed to different mechanisms such as chromosomal alterations of the miRNA genes (amplification, deletion, or mutation), epigenetic changes (DNA methylations and histone acetylations), and alterations in the biogenesis machinery [84]. miRNAs are involved in several cancer-related processes such as proliferation, migration, invasion, and apoptosis, in addition to their role in regulating cancer stem cells (CSCs) formation and epithelial to mesenchymal transition (EMT) [85]. Several studies have shown that miRNA expression profiles can distinguish between normal and cancerous tissues, specify the origin of tumor, and discriminate between the different subtypes of a specific cancer type [49, 86]. Besides, miRNAs can predict cancer outcome and response to therapy and is an important indicator of drug resistance [87, 88]. These findings highlight their importance as diagnostic, prognostic, and therapy predictive biomarkers.

Owing to their characteristics, miRNAs have been reported to be novel potential non-invasive biomarkers for cancer and other diseases [89, 90]. The presence and stability of miRNAs in several biological fluids, including blood plasma, serum, saliva, and urine, in addition to the easiness of their detection, make miRNAs useful biomarkers for cancer diagnosis, prognosis, and therapy prediction [91]. For example, miR-21 has been shown in multiple studies to serve as a biomarker for early BC diagnosis. It was significantly upregulated in the plasma and serum of BC patients compared to normal controls [89, 92, 93].

4. miRNAs and Breast Cancer

The dysregulation of miRNAs in BC was first reported in 2005 by Iorio et al. They have shown that miRNAs (including miR-125b, miR-145, miR-21, and miR-155, the most significantly dysregulated ones) were aberrantly expressed in human breast tissues compared to normal ones [94]. Subsequently, miRNAs have been shown to be differentially expressed between the different subtypes of BC. Mattie et al. have shown that distinct miRNA subsets distinguish HER2+ from ER+, HER2+ from HER2-, and ER+ from ER- breast cancers. A subset of miRNAs (including miR-107, miR-153, and miR-195) was specific to HER2 status while a different subset (including miR-142-5p, miR-205, and miR-25) was specific to ER/PR status [95]. Then, Blenkiron et al. reported a large number of miRNAs to be differentially expressed between the different molecular BC subtypes thus, suggesting that miRNA profiling can be utilized to classify the molecular BC subtypes. For instance, miR-20a, miR-106a, and miR-17-5p were differentially expressed in basal-like subtype whereas, miR-10a and miR-10b were differentially expressed in Luminal A subtype [96]. Recently, Bhattacharyya et al. reported the differential expression of several miRNAs in different combinations of BC samples. They clustered the tumor samples according to the miRNA expression profiles and concluded that there is a high number of miRNAs differentially expressed in a particular cluster whereas others (like miR-124 and miR-483-3p) were expressed in almost all the clusters thus, suggesting that miRNA profiling can be utilized to determine BC subtypes. [97]. Accordingly, miRNA profiling might be superior to mRNA profiling in the classification

of BC, which would eventually contribute to developing new prognosis predictors and novel approaches for treating BC.

Several studies have shown that different cellular pathways of BC development are regulated by either oncogenic or tumor suppressor miRNAs. These include cell cycle progression and proliferation, apoptosis, migration and invasion, angiogenesis, EMT, in addition to BC stem cells and tumor microenvironment regulation, and drug resistance [98]. For example, miR-492 was shown to be upregulated in BC tissues compared to adjacent non-tumor tissues, and its overexpression in BC cell lines promoted cell proliferation and upregulated the levels of cyclin D1 and c-Myc that are involved in cell cycle progression [99]. Moreover, miR-140-5p was reported to be downregulated in BC tissues, and its overexpression inhibited tumor invasion and angiogenesis by targeting VEGF-A [100]. In addition to their roles in breast tumorigenesis, miRNAs can also act as potential diagnostic, prognostic, and therapy predictive biomarkers, which might help us detect early breast cancer (EBC) and improve therapy outcomes. For example, miR-155 was shown to be significantly upregulated in the sera of BC patients, thus, making it a diagnostic biomarker for EBC [101, 102]. Multiple studies have reported miRNAs as prognostic biomarkers for EBC. Upregulated miR-9 in BC tissues, especially ER+ tissues, was associated with poor overall survival and local recurrence [103]. miRNAs could also have a therapy predictive role in BC. Several dysregulated miRNAs were correlated with resistance or sensitivity to radiotherapy, chemotherapy, hormonal, and targeted therapy. For instance, increased levels of miR-210 in HER2+ patients were associated with resistance to trastuzumab [104].

5. miRNAs and Lebanese Breast Cancer Patients

As mentioned previously, BC is the most common and the deadliest type of cancer among Lebanese women. In 2014, Nassar et al. have reported for the first time miRNA expression patterns in Lebanese BC tissues. They found that specific miRNAs (miR-148b, miR-10b, miR-21, miR-221, miR-155) that are previously reported to be differentially expressed in BC, are differentially expressed (except for miR-221) in Lebanese BC tissues as compared to normal adjacent tissues (NAT). However, the expression of some of these miRNAs, miR-148b and miR-221, differed from those reported in the West, indicating that miRNA expression could vary between Lebanese and Western populations [105]. Therefore, this study showed the necessity of conducting a global miRNA microarray analysis to identify specific miRNA signatures in Lebanese BC patients. This was done in 2017, where they have reported the significant dysregulation of 173 mature miRNAs in Lebanese BC tissues as compared to NAT, with 21 miRNAs exclusively dysregulated in Lebanese patients (for example, miR-31 and miR-663) and 4 miRNAs having different expression patterns (example miR-324-3p) in comparison with matched American patients. Of these miRNAs, miR-126 was significantly downregulated [106].

6. miR-126

In the human genome, miR-126, an endothelial-specific miRNA, is located on chromosome 9 within the seventh intron of the epidermal growth factor-like domain 7 (EGFL7) gene. miR-126 has been reported to be expressed in highly vascularized tissues, such as the heart and lungs, where it plays a crucial role in angiogenesis and maintaining

vascular integrity [107]. The mature form is known as miR-126-3p, usually referred to as miR-126, for it is excised from the 3' side of the precursor hairpin. miR-126-5p, also known as miR-126*, is the analogous anti-sense strand to miR-126-3p that has less known functions in regulating gene expression [108]. Aberrant expression of miR-126 has been described in several solid and hematologic tumors. miR-126 is commonly downregulated in most cancers, such as lung, pancreatic, colorectal, esophageal, and other cancers, and shows tumor suppressive properties. In addition, its downregulation acts as a significant predictor of poor survival in many cancers [109]. miR-126 inhibits tumor progression by reducing proliferation, migration, invasion, and angiogenesis via altering the levels of multiple mRNA targets (Table 3). For example, miR-126 overexpression in prostate cancer cells inhibits proliferation, migration, and invasion of cells *in vitro*, through targeting ADAM9 mRNA [110]. However, in some cases, miR-126 enhances cancer progression. This is observed in acute myeloid leukemia (AML), where miR-126 levels are reported to be upregulated in patients with AML [111]. Moreover, its inhibition induced apoptosis and repressed cell proliferation via targeting TRAF7 in AML [112].

In breast cancer, some studies have shown that miR-126 is downregulated in BC tissues as compared to adjacent normal ones [113, 114]. Moreover, miR-126 expression was shown to be significantly lower in basal-like BC tissues than in non-basal-like ones. Higher levels of miR-126 were associated with favorable TNBC outcomes (better disease-free survival (DFS) and overall survival (OS)) [115]. A genome wide study reported that miR-126 is overexpressed in patients with DCIS when compared to patients with IDC. Add to this, higher levels of miR-126 were associated with better prognosis in IDC patients,

reiterating that this miRNA down-modulates invasive properties, as shown in *in vitro* studies [116]. Recently, miR-126 downregulation was shown to be associated with the absence of estrogen receptor in BC tissues, whereas no association with HER2 status was observed [114]. This correlation might be further studied to decipher the mode of action of miR-126 and ER. In addition, low expression of miR-126 was found to be associated with BC metastasis [117, 118]. Loss of miR-126 expression in primary breast tumors was associated with poor distal metastasis-free survival. *In vivo*, miR-126 restoration decreased overall tumor growth and metastasis to lungs and bones [118]. Hence, the mentioned effects of miR-126 in different types of cancer in general and in BC in specific stimulated our interest to elucidate further the role of miR-126 in BC tumorigenesis.

Table 3. Summary of miR-126 Expression and Role in Different Types of Cancer

Cancer Type	miR-126 Expression	Significance	Targets	References
Colorectal cancer	Downregulated in tissues and cell lines	Suppresses cell viability, growth, proliferation, migration and invasion, induces cell cycle arrest at G0/G1 phase, autophagy, and apoptosis, inhibits growth and metastasis in vivo	CXCR4, IRS1, SLC7A5, TOM1, VEGF, PIK3R2, RhoA/ROCK pathway, AKT and ERK1/2 pathway, mTOR	X. Li et al. 2011, N. et al. 2013, Z. Li et al. 2013, Zhang et al. 2013, Guo et al. 2008, Lui et al. 2013, Zhou et al. 2013, Wei et al. 2020, Yuan et al. 2015, Ebrahimi et al. 2015
Gastric cancer	Downregulated in tissues and cell lines (SGC-7901, NCI-N87, MKN-45, MKN-28, BGC-823, SNU-16, AGS, SNU-1, KATO III)	Reduces cell proliferation by inducing cell cycle arrest in G0/G1 phase, migration, invasion, and angiogenesis in vitro, and carcinogenesis, metastasis, and angiogenesis in vivo	CRK, CRKL, SLC7A5, VEGF-A, SRPK1	Feng et al. 2010, Wang et al. 2013, Wang et al. 2015, Chen et al. 2014, Li et al. 2014, Li et al. 2018
	Upregulated in tissues and cell lines (HSC43, NUGC3, GCIY, NUGC4, HSC58)	Enhances proliferation and colony formation	SOX2	Otsubo et al. 2011
	Downregulated in tissues and cell lines (SGC-7901, BGC-823)	Suppresses proliferation in vitro and in vivo, colony formation, induces apoptosis	PI3KR2, CRK, PLK2	Lui et al. 2014
Glioma	Downregulated in tissues and cell lines	Inhibits cell proliferation, colony formation, migration, invasion, induces cell cycle arrest at G0/G1 phase and apoptosis, inhibits tumor growth in vivo	IRS1, PI3K/AKT pathway, GATA4, MTCP1, KRAS, PTEN/PI3K/AKT pathway, MDM2-p53 pathway	Luan et al. 2015, Xu et al. 2016, Han et al. 2018, Li et al. 2015, Chen et al. 2019
Esophageal cancer	Downregulated in tissues and cell lines	Inhibits cell proliferation, migration, invasion, and colony formation, suppresses G2/M phase transition, inhibits growth in vivo	PIK3R2, VEGF-A, IRS1, GOLPH3, ADAM9	Hu et al. 2011, Nie et al. 2015, Kong et al. 2016, Li et al. 2014, Lui et al. 2014
Oral carcinoma	Downregulated in tissues and cell lines	Inhibits angiogenesis and lymphangiogenesis, inhibits cell migration, invasion, proliferation, G1 phase transition, colony formation, and induces apoptosis	VEGF-A, ADAM9, EGFL7, KRAS	Sasahira et al.2012, Qin et al. 2019, Yang et al. 2014, Han et al. 2016

Cancer Type	miR-126 Expression	Significance	Targets	References
Pancreatic cancer	Downregulated in tissues and cell lines	Reduces cell migration, invasion, and induction of the epithelial marker E-cadherin	ADAM9, KRAS, CRK	Hamada et al. 2012, Jiao et al. 2012
Hepatocellular carcinoma	Downregulated in tissues and cell lines	Inhibits cell proliferation, migration, invasion, G1 phase transition, and colony formation, promotes apoptosis, suppresses growth and lung colonization in vivo, suppresses angiogenesis in vitro and in vivo	LRP6, PIK3R2, EGFL7, PLK4, SOX2, SPRED1	Han et al. 2012, Chen et al. 2013, Du et al. 2014, Hu et al. 2016, Bao et al. 2018, Zhao et al. 2015, Ji et al. 2016
Thyroid cancer	Downregulated in tissues and cell lines	Inhibits proliferation in vitro and in vivo, tumor growth and lung metastasis in vivo, colony formation, angiogenesis, migration, and invasion, promotes apoptosis and cell cycle arrest at G1 phase	CXCR4, SLC7A5, ADAM9, LRP6, VEGF-A, PIK3R2	Kitano et al. 2011, Qian et al. 2016, Xiong et al. 2015, Wen et al. 2015, Salajegheh et al. 2015, Rahman et al. 2015
Cervical cancer	Downregulated in tissues and cell lines	Inhibits angiogenesis, migration, and invasion	ADM, ZEB1	Wang et al. 2008, Huang et al. 2014, Xu et al. 2019, Yu et al. 2013
Bladder cancer	Downregulated in tissues and cell lines	Inhibits proliferation, colony formation, migration, invasion, G1 phase transition, and promotes apoptosis	ADAM9, PI3KR2	Saito et al. 2009, Jia et al. 2014, Xiao et al. 2016
Prostate cancer	Downregulated in tissues and cell lines	Inhibits proliferation, migration, and invasion	ADAM9	Saito et al. 2009, Hua et al. 2016
	Upregulated in metastatic xenograft line	-	-	Watahiki et al. 2011
Renal carcinoma	Downregulated in tissues and cell lines	Inhibits cell growth, proliferation, migration, and invasion, induces arrest at G0/G1 phase	IRS1, VEGF-A, ROCK1, SLC7A5	Zhang et al. 2008, Khella et al. 2012, Zhang et al. 2016, Lui et al. 2017
Osteosarcoma	Downregulated in tissues and cell lines	Inhibits cell growth, proliferation, migration, invasion, and EMT, induces cell cycle arrest at G0/G1 phase	Sirt1, ADAM9, ZEB1	Xu et al. 2013, Wang et al. 2015, Jiang et al. 2014, Jiang et al. 2017
Endometrial cancer	Downregulated in tissues and cell lines	Inhibits migration and invasion	IRS1	Zhao et al. 2015

Cancer Type	miR-126 Expression	Significance	Targets	References
Lung cancer	Downregulated in tissues and cell lines	Inhibits proliferation, colony formation, adhesion, migration, and invasion, induces cell cycle arrest at G1, inhibits growth and metastasis in vitro and in vivo	CRK, VEGF-A, EGFL7, PI3KR2, SLC7A5, CCR1, PTEN/PI3K/AKT pathway, PI3K/AKT/Snail pathway	Crawford et al. 2008, Liu et al. 2009, Sun et al. 2010, Yang et al. 2012, Miko et al. 2011, Yang et al. 2015, Liu et al. 2019, Song et al. 2016
Mesothelioma	Downregulated in tissues	Inhibits cell growth and colony formation, promotes cell cycle arrest at G0/G1 phase, inhibits tumor growth in vivo, and induces autophagy	IRS1	Santarelli et al. 2011, Tomasetti et al. 2014, Tomasetti et al. 2016
Melanoma	Downregulated in metastatic cell lines, upregulated in primary cell lines	Reduces proliferation, invasion, and chemotaxis in vitro, reduces growth and dissemination in vivo	ADAM9, MMP7	Felli et al. 2013
Leukemia	Upregulated in acute myeloid leukemia samples and cell lines	Inhibits apoptosis, increases viability, growth, proliferation, colony formation, and differentiation, increases self-renewal of AML LSCs	PLK2, HOXA9, TRAF7	Li et al. 2008, Cammarata et al. 2010, Leeuw et al.2014, Lechman et al. 2016, Ding et al. 2018
	Downregulated in adult T cell leukemia	-	-	Ishihara et al. 2012
	Upregulated in B cell acute lymphoblastic leukemia	Inhibits senescence, cell cycle arrest, and apoptosis in vivo	p53 pathways	Nucera et al. 2016
Myeloma	-	Reduces cell viability, inhibits growth, and induces apoptosis	MCL	Lui et al. 2018
Ovarian cancer	Downregulated in tissues and cell lines	Induces cell cycle arrest at G1 phase, suppresses cell proliferation, migration, invasion, and promotes apoptosis, inhibits tumor growth in vivo	VEGF, PLXNB2, AKT and ERK1/2 pathway, PAK4, EGFL7	Luo et al. 2017, Xiang et al. 2018, Luo et al. 2015, Tu et al. 2019
Kaposi's sarcoma	Upregulated in tissues	Inhibits cell proliferation and invasion, promotes apoptosis and cell cycle arrest at G2/M phase	PIK3R2, PTEN/PI3K/AKT pathway	Wu et al. 2014, Wu et al. 2016, Lu et al. 2018

C. Aim of the Study

Recently, our group has shown a panel of miRNA dysregulated in Lebanese BC tissues by conducting microarray profiling analysis. Of these miRNAs, miR-126 was significantly downregulated. Since there is a discrepancy in the reported functions of miR-126 in BC proliferation and mammospheres formation we will conduct this study to better understand its role in BC tumorigenesis mediated through different mRNA targets that were not validated previously in BC. Aberrant expression of miR-126 in Lebanese BC tissues was validated using real time PCR (RT-qPCR). Different functional assays will be done to determine the role of the dysregulated miR-126 in cell proliferation, cell cycle progression, and colony formation in BC cell lines (MCF-7 and MDA-MB-231) and non-tumorigenic cell line (MCF-10A). *In silico* analysis will be done to determine the potential targets of the corresponding miRNA; those that are involved in BC tumorigenesis will be selected. We will assess the effects of modulating the expression of miR-126 on the predicted targets by RT-qPCR, where we will focus on the most altered target mRNA for further studies. Finally, *in silico* Kaplan-Meier analysis will be done to determine the prognostic role of miR-126 in BC patients. As such, this study will unveil the role of miR-126 as a potential player in BC development.

CHAPTER II

MATERIALS AND METHODS

A. Cell Culture

BC cell lines MCF-7 (ER+, PR+, HER2-) and MDA-MB-231 (ER-, PR-, HER2-) were maintained in Dulbecco's Modified Eagle's Medium (DMEM) high glucose (Sigma Aldrich) with 10% Fetal Bovine Serum (FBS) (Sigma Aldrich), 1% sodium pyruvate, 1% penicillin/streptomycin, and 0.5% kanamycin. Non-tumorigenic epithelial cell line MCF-10A was maintained in DMEM F12 (Sigma Aldrich) with 5% Horse Serum (STEM CELL Technologies), 20 ng/ml Epidermal Growth Factor (EGF), 0.5 µg/ml hydrocortisone, 100 ng/ml choleratoxin, 10 µg/ml insulin, and 1% penicillin/streptomycin. Cells were incubated at 37ºC with 5% CO_2.

B. Transfection of the Cells

300,000 cells of MCF-10A, 500,000 cells of MCF-7, and 280,000 cells of MDA-MB-231 were seeded per well in a 6-well plate for the different assays. Cells were seeded in duplicates per condition: untransfected or control cells (CTL), cells transfected with miR-126 mimic to increase miR-126 levels, and cells transfected with negative control (NC) duplex to rule out the effect of the transfection process (GenePharma, Shanghai), all of which were FAM-labeled. 5,000 cells per well were seeded in triplicates per condition in a 96-well plate for the MTT assay, one plate for each time point (24, 48, and 72 hours). Cells were incubated overnight to reach 60-80% confluency. Media was replenished with

antibiotic free media 2 hours before transfection. Transfection using Lipofectamine RNAiMAX Reagent (Invitrogen) and Opti-MEM Medium (Gibco) was done according to the manufacturer's instructions. For the 6-well plates, both lipofectamine and 30pmol of the mimic/NC were diluted in 150µl Opti-MEM. After incubation for 5 minutes at room temperature (RT), diluted mimic/NC was added to diluted lipofectamine in a 1:1 ratio and incubated for 10 minutes at RT. 250µl per well of each complex was then added drop by drop in a circular pattern to ensure proper dispersion of the lipid complex. Cells were incubated and harvested after 24 or 48 hours. Media was removed, wells were washed with 1ml of 1x Phosphate Buffered Saline (PBS) (Lonza), 500µl Trypsin-EDTA (Sigma Aldrich) was added per well for 20 seconds in the humidified incubator, then neutralized with 1ml cDMEM. Cells were collected at 900rpm for 3 minutes and stored at -80ºC for RNA extraction and RT-qPCR analysis or processed directly for specific functional assays. For the 96-well plates, both lipofectamine and 5pmol of the mimic/NC were diluted in 25µl Opti-MEM then, 10µl of the final complex was added per well. Plates were incubated for 24, 48 and 72 hours to perform MTT assay.

Table 4. The Sequences of miR-126 Mimic and the Negative Control Duplex

Component	**Sense (5'-3')**	**Antisense (5'-3')**
hsa-miR-126 mimic	UCGUACCGUGAGUAAUAAUGCG	CAUUAUUACUCACGGUACGAUU
Negative control duplex	UUCUUCGAACGUGUCACGUTT	ACGUGACACGUUCGGAGAATT

C. Total RNA Extraction

Transfected cells were harvested 24 hours post transfection for RNA extraction and RT-qPCR analysis. Total RNA was extracted from the cells using TRI Reagent (Sigma Aldrich) according to the manufacturer's instructions. 1ml of TRI Reagent was added per sample, and samples were incubated for 5 minutes at RT to ensure that cells are totally lysed. Then, 200µl of chloroform was added per 1ml TRI Reagent, mixed by inverting for 15 seconds, and centrifuged at 12,000xg for 15 minutes at 4ºC. The mixtures separate into a lower red phenol-chloroform phase, a DNA rich interphase, and a colorless upper aqueous phase that contains the RNA. The tubes were angled at 45º, and the aqueous phases were transferred into new tubes. 500µl of 100% isopropanol was added per 1ml TRI Reagent, vortexed for 2 seconds, and incubated at RT for 10 minutes. Samples were then centrifuged at maximum speed (21,100xg) for 15 minutes at 4ºC to collect the RNA. The supernatants were removed without disturbing the RNA pellets. Two steps of washing with 75% ethanol prepared in DEPC water were done. Each step was followed by centrifugation at 7,500xg for 5 minutes at 4ºC. Pellets were air dried for at least 10 minutes to ensure that there is no residual ethanol. Then, pellets were resuspended in 40µl DEPC (RNase-free) water and incubated for 15 minutes at 55ºC on a heat block. The optical density (260 nm) of each sample (of volume 2µl) was read using Denovix DS11 Spectrophotometer (AGBL). For each sample, the ratio 260/280 was between 1.8 and 2.1, and DEPC water was used as a blank. Samples were stored at -80ºC for later use in cDNA synthesis. RNA quality was also assessed by gel electrophoresis (1% agarose gel was prepared).

D. miRNA Expression by Reverse Transcription Quantitative Real Time PCR (RT-qPCR)

Reverse transcription of 10ng of RNA was performed using TaqMan® microRNA Reverse Transcription Kit (Applied Biosystems). Multiplex cDNA master mixes were prepared on ice. 3µl of DEPC treated water, 0.1µl of 100mM dNTPs, 1µl of 10x Reverse Transcriptase Buffer, 0.13µl of RNase Inhibitor, 0.67µl of Multiscribe Reverse Transcriptase enzyme, and 1µl of each 5x microRNA primers (RNU6B as an endogenous control and miR-126), for a total volume of 6.9µl, were added per reaction sample. 3.1µl of the 10ng RNA diluted in DEPC was added to each reaction tube on ice. Reaction samples were well mixed and loaded in the BioRad T100 thermal cycler. The protocol is as follows: 30 minutes incubation at 16ºC, 30 minutes incubation at 42ºC, 5 minutes incubation at 85ºC, and infinite hold at 4ºC. cDNA samples were diluted by adding 57µl DEPC water and stored at -20ºC for later use in RT-qPCR.

RT-qPCR for miR-126 expression was performed using TaqMan® microRNA Assays and 2x TaqMan® Universal Master Mix with no Amperase Uracil N-glycosylase (UNG) (Applied Biosystems). The master mixes were prepared as follows: 5µl of 2x Universal Master Mix, 0.5µl of the corresponding 20x microRNA probe, and 2µl of DEPC water. 7.5µl of the master mix followed by 2.5µl of each cDNA sample were distributed in each reaction well of a BioRad 96 well skirted PCR plate. No template control (NTC) reaction well with no cDNA template was included as well. Plate was spun briefly at 2,500xg for 1 minute and then loaded into the qPCR BioRad CFX96 machine. The following steps were run: 10 minutes hold at 95ºC, 40 cycles of 15 seconds at 95ºC

(denaturing step), and 60 seconds at 60ºC (annealing and extension step). miR-126 expression was normalized against the endogenous control RNU6B. Using the ΔΔCq, the relative expression of miR-126 was determined in the miR-126 mimic transfected cells compared to the NC transfected cells.

Table 5. Probe Sequences of miR-126 and the endogenous control RNU6B

microRNA	**Probe Sequence**
RNU6B	CGCAAGGATGACACGCAAATTCGTGAAGCGTTCCATATTTTT
hsa-miR-126	UCGUACCGUGAGUAAUAAUGCG

E. Transfection Efficiency

Cells were transfected and harvested as previously described. Then, cells were resuspended in 1ml of 1x PBS. 100µl per condition were transferred to 1.5ml Eppendorf tubes and resuspended with another 200µl of 1x PBS. Cells were analyzed on Guava EasyCyte8 Flow Cytometer (Millipore) to determine the transfection efficiency. Fluorescence intensity was adjusted upon loading the untransfected control sample. Green Fluorescence (GRN-HLog) versus Side Scatter (FSC-HLin) was measured, and 10,000 events were collected. The percentages of transfected cells were quantitated by the software. The remaining 900µl were stained for cell cycle analysis.

F. Cell Growth/MTT Assay

Cells were transfected as previously mentioned. 24, 48 and 72 hours post transfection, 10µl of 5mg/ml MTT (3-[4,5-dimethylthiazol-2-yl]-2,5 diphenyl tetrazolium bromide) was added per well. Plates were incubated at 37ºC with 5% CO_2 for 3 hours then,

100µl of stop solution was added per well. The next day, absorbance was measured at 595nm by TriSTAR^2 S LB 942 Multimode Reader (Berthold Technologies).

G. Cell Cycle Analysis

Transfected cells were harvested 24 and 48 hours post transfection. 900µl per condition were transferred to 1.5ml Eppendorf tubes. Cells were centrifuged at 2,000rpm for 10 minutes (for the rest of the protocol). Supernatant was discarded, and cells were fixed by resuspending the pellets in 1ml of cold 70% ethanol (prepared in 1x PBS). Fixed cells are stored at -20ºC. On the day of the experiment, ethanol was removed by spinning down the fixed cells. Cells were then washed with 1ml of 1x PBS, centrifuged, and treated with 100µl per pellet of Ribonuclease (RNase, working concentration = 0.2mg/ml) to make sure that only the DNA is stained. Samples were incubated at 37ºC for 40-50 minutes then centrifuged to get rid of the RNase. Cells were then resuspended in 200µl of 1x PBS + 20µl of Propidium Iodide staining (PI, working concentration = 1mg/ml). Samples were mixed thoroughly and incubated at 4ºC for 45 minutes protected from light. Then, 200µl of 1x PBS was added per sample. Samples were analyzed on Guava EasyCyte8 Flow Cytometer (Millipore). Cell cycle of the total cell count was measured by plotting Red Fluorescence Area (RED-HLin) versus Red Fluorescence Width (RED-W), and 10,000 events were collected. Singlet cells (<5,000) were gated. DNA peaks of G0/G1 and G2/M were adjusted by loading the untransfected control sample. The percentages of cells in each cell cycle phase were quantitated by the software. To gate for the transfected cells, green fluorescence was measured simultaneously with red fluorescence.

H. Colony/Sphere Formation Assay

Cells were seeded and transfected as previously described. After 48 hours, cells were harvested as follows. Culture media was aspirated then, cells were rinsed twice with 1ml of Hank's Balanced Salt Solution (HBSS) (Lonza) to remove residual media from the wells. Using a sterile scraper, cells were scraped gently. Scraped cells were resuspended in 2ml of MammoCult™ media (STEM CELL Technologies) with 10% MammoCult™ Proliferation Supplement (STEM CELL Technologies), 0.2% heparin, and 0.5% hydrocortisone, and transferred to 15ml conical tubes. Cells were centrifuged at 500xg for 3 minutes then, supernatant was aspirated carefully. Pellets were resuspended in 1ml of cMammoCult then counted using Trypan Blue. 40,000 cells/well of MCF-7 and 5,000 cells/well of MDA-MB-231 per condition were seeded in 2ml cMammoCult in low adherent 6-well culture plates and incubated for 7 days. After 7 days, spheres were counted and passaged as follows. Media was aspirated and centrifuged at 100xg for 5 minutes to harvest the spheres. Supernatant was aspirated carefully, and spheres were resuspended in 500µl cMammoCult. 50µl of each suspension was added to a 96-well plate marked at its backside into a quadrant. Spheres were then counted in each quadrant and the total number of spheres was calculated as follows: Total number of spheres = (number of counted spheres/counting volume) × total volume. To passage the spheres, the suspension was centrifuged at 350xg for 5 minutes then, the supernatant was aspirated carefully. 500µl of pre-warmed Trypsin-EDTA was added for 1 minute at RT. Then, 800µl of cMammoCult was added to deactivate Trypsin. Mammospheres were broken by tilting the tip and pressing it against the bottom and side of the tube for 1-2 minutes to generate resistance to

break up the spheres. 5ml of HBSS + 2% of FBS was added then, cell suspensions were centrifuged at 350xg for 5 minutes. Supernatant was aspirated carefully, and pellets were resuspended with 0.5ml cMammoCult. Cells were counted using Trypan Blue and seeded according to the previously mentioned densities. Carl Zeiss ZEN image software was used for the acquisition of bright field images of the mammospheres.

I. *In Silico* Predicted and Experimentally Validated Target Databases and *In Silico* Kaplan-Meier Analysis

Two predicted target databases microT-CDS (Diana Tools) and TargetScanHuman 7.2, and an experimentally validated database Tarbase 7.0 (Diana Tools) were utilized to search for predicted mRNA targets of miR-126. PubMed search was performed to check for validated miRNA-mRNA interaction in BC and other types of cancer, in addition, to check the role of the resulting mRNA targets in BC.

miRpower web-tool was utilized to determine the survival of patients with dysregulated miR-126 or SLC7A5 expression. Meta data for Kaplan–Meier survival analysis were obtained from https://kmplot.com/analysis/index.php?p=service&cancer=breast_mirna and https://kmplot.com/analysis/index.php?p=service&cancer=breast. Patients with ER+ status were selected from the METABRIC database. Kaplan–Meier plots were generated and a p-value <0.05 was considered as a significant correlation between miRNA/target expression and survival.

J. Primers Optimization of the Selected mRNA Targets

Primers of the selected mRNA targets genes were designed on PrimerBank. The specificity, amplicon size, and melting temperature (Tm) were checked on PrimerBlast. Primers were optimized on untransfected MCF-7 or MDA-MB-231 cells. RNA was extracted as previously mentioned.

1. cDNA Synthesis for mRNA Expression

Reverse transcription of 1000ng of RNA was performed using the iScript™ cDNA Synthesis Kit (Bio-Rad). cDNA master mixes were prepared on ice. 4µl of 5x iScript Reaction Mix and 1µl of iScript Reverse Transcriptase were added to a total of 15µl of 1000ng RNA diluted in DEPC water. No Reverse Transcriptase sample (NRT) was included as a negative control. Reaction samples were well mixed and loaded in the BioRad T100 thermal cycler. The following steps were run: 5 minutes incubation at 25ºC (priming), 20 minutes incubation at 46ºC (reverse transcription), 1 minute incubation at 95ºC (RT inactivation), and infinite hold at 4ºC. cDNA samples were diluted by adding 20µl DEPC water and stored at -20ºC for later use in RT-qPCR.

2. Primers Optimization by RT-qPCR

Different concentrations of the primers were tested for optimization. The master mixes were prepared as shown in Table 6. 9µl of each master mix followed by 1µl of the cDNA sample were distributed in each reaction well of a BioRad 96 well skirted PCR plate. NRT and NTC reaction wells were also included. Plate was spun briefly at 2,500xg

for 1 minute and then loaded into the qPCR BioRad CFX96 machine. The following steps were run: 10 minutes hold at 94ºC, 40 cycles of 15 seconds at 94ºC (denaturing step), 60 seconds at 60ºC (annealing and extension step), as well as a melt curve 55ºC to 95ºC with an increment 0.5ºC for 0.05 seconds. The optimal concentration per primer was selected based on the highest melting peak. Size of the products were checked by gel electrophoresis (2% agarose gel was prepared). Primers that did not show a clear peak on 60ºC were tried on a temperature gradient to choose the most suitable temperature.

Table 6. Primers Optimization performed on different concentrations and temperatures

Primers (nM)	**100**	**200**	**300**	**400**	**500**
SYBR (µl)	5	5	5	5	5
PF (µl)	0.1	0.2	0.3	0.4	0.5
PR (µl)	0.1	0.2	0.3	0.4	0.5
DEPC (µl)	3.8	3.6	3.4	3.2	3
cDNA (µl)	1	1	1	1	1
Total (µl)	10	10	10	10	10

K. Gene Expression of the Selected mRNA Targets by RT-qPCR

cDNA was synthesized as previously described. RT-qPCR for targets expression was performed using iTaq^{TM} Universal SYBR Green® Supermix (BioRad). The master mixes were prepared depending on the selected concentration of each primer (Table 6). The same procedure and protocol were run as previously described. mRNA expression was normalized against the housekeeping gene GAPDH. Using the ΔΔCq, the relative expression of the mRNA targets was determined in the miR-126 mimic transfected cells compared to the NC transfected cells.

L. Statistical Analysis

Statistical analysis was performed using GraphPad Prism 7 Software. Student's *t*-test was used to analyze differences between the two groups. Data presented are the means ± SEM of two, three, or four different experiments as noted in the figure legends. A p-value <0.05 was considered statistically significant (*P<0.05, **P<0.01, ***P<0.001).

CHAPTER III

RESULTS

1. miR-126 Expression in Lebanese BC Patients

Previously, our group performed miRNA microarray analysis to identify specific miRNA signatures in Lebanese BC patients. The microarray analysis was performed on RNA extracted from formalin fixed paraffin embedded (FFPE) sections from 45 invasive ductal carcinoma specimens and 17 normal adjacent tissues (NAT). It revealed a total of 173 mature miRNAs that were significantly dysregulated, of which 74 miRNAs were differentially expressed with a fold change (FC) more than 2. Of these 173 dysregulated miRNAs, miR-126 was significantly downregulated in patients of all ages and in patients above the age of 40 with FC<2, and it was significantly downregulated in patients below the age of 40 with FC>2 (Table 7).

Table 7. Microarray Analysis of miR-126 in Lebanese BC Tissues

hsa-miR-126	logFC	FC	adj.P.value	Mode of Dysregulation
All	-0.77	1.7	0.00016	downregulated
Above 40	-0.69	1.61	0.01	downregulated
Under 40	-1.10	2.14	0.0196	downregulated

To further validate the dysregulation of miR-126, our group performed RT-qPCR on 15 tumors and 9 NAT. When analyzing miRNA expression in all tumor patients (<40 and >40 years combined) as compared to NAT, they found that miR-126 was significantly downregulated in tumor patients with p=0.0001. Upon analyzing miRNA expression in

different age groups (<40 years or >40 years) as compared to NAT, results have shown that miR-126 was significantly downregulated in both <40 years and > 40 years ($p<0.05$) (Figure 6).

Based on these results, we were interested to further explore the role of miR-126 in BC tumorigenesis. So, the following study was conducted.

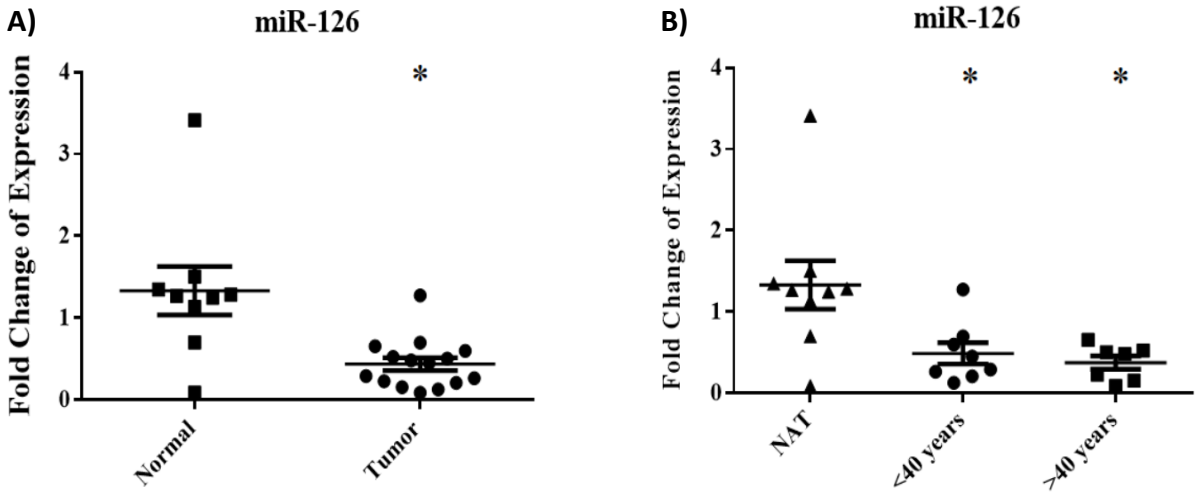

Figure 6. Validation of miR-126 Dysregulation in Lebanese BC Tissues versus NAT by RT-qPCR. Dot plots show the fold change of miR-126 in 15 (A) and in 8 <40 years and 7 >40 years (B) patient breast cancer tissues normalized to the average of 9 NAT with RNU6B used as an endogenous control. Error bars represent SEM. * denotes $p<0.05$ for tumor versus NAT using Wilcoxon's signed-rank sum test.

2. miR-126 Expression in BC Cell Lines

In order to study the role of miR-126 in BC, RT-qPCR was utilized to determine the relative expression of miR-126 in the BC cell lines MCF-7 and MDA-MB-231 in comparison to the non-tumorigenic epithelial cell line MCF-10A with RNU6B used as an endogenous control. Both MCF-7 and MDA-MB-231 showed significant upregulation of miR-126 compared to the non-tumorigenic cell line MCF-10A (Figure 7).

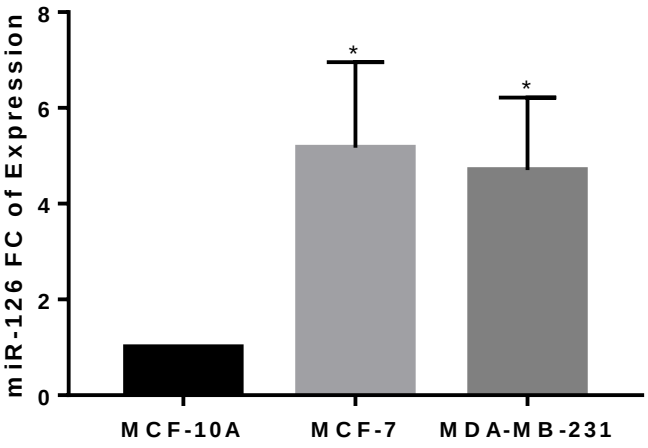

Figure 7. Endogenous Expression Levels of miR-126 in MCF-7 and MDA-MB-231 compared to MCF-10A. RNU6B was used as an endogenous control. Error bars represent SEM (n=3). * denotes $p<0.05$.

3. miR-126 Overexpression in BC and Non-tumorigenic Cell Lines upon Transfection with miR-126 FAM-labeled Mimic

To explore the role of miR-126 in BC, the non-tumorigenic cell line MCF-10A and the BC cell lines MCF-7 and MDA-MB-231 were transfected with FAM-labeled miR-126 mimic and NC duplex. Transfection efficiency was validated by flow cytometry for miR-126 mimic and NC duplex transfected cells as compared to CTL 24 hours post transfection (Figures 8A, 9A, 10A). All cell lines were significantly transfected with miR-126 mimic, with a mean percentage of 47.36% in MCF-10A ($p=0.022$) (Figure 8B), 71.31% in MCF-7 ($p=0.0006$) (Figure 9B), and 72.62% in MDA-MB-231 ($p=0.0049$) (Figure 10B) compared to the CTL. Then, miR-126 levels were detected in cells transfected with miR-126 mimic as compared to NC duplex transfected cells 24 hours post transfection by RT-qPCR with RNU6B used as an endogenous control. miR-126 was

significantly overexpressed in MCF-10A ($p=0.044$) (Figure 8C), MCF-7 ($p=0.0002$) (Figure 9C), and MDA-MB-231 cells ($p<0.0001$) (Figure 10C) transfected with miR-126 mimic as compared to NC.

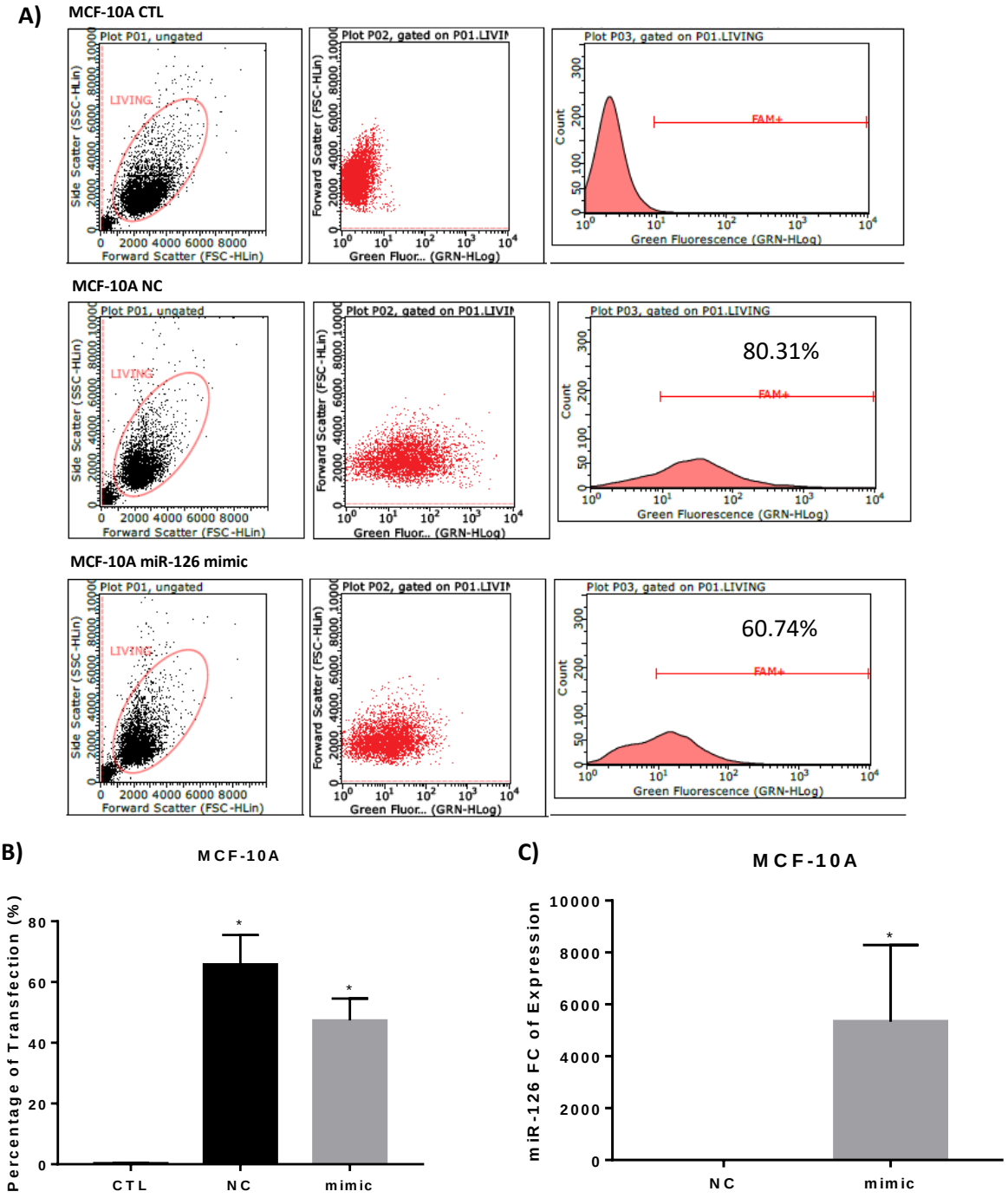

Figure 8. Transfection Efficiency of miR-126 mimic in MCF-10A. Transfection efficiency was measured by flow cytometry and RT-qPCR in MCF-10A 24hrs post transfection. (A): Representative figures of flow cytometric analysis of miR-126 mimic and NC transfected cells as compared to CTL, (B): Percentage of miR-126 mimic and NC transfected cells as compared to CTL, (C): RT-qPCR analysis of miR-126 levels as compared to NC, RNU6B was used as an endogenous control. Error bars represent SEM (n=3). * denotes $p<0.05$.

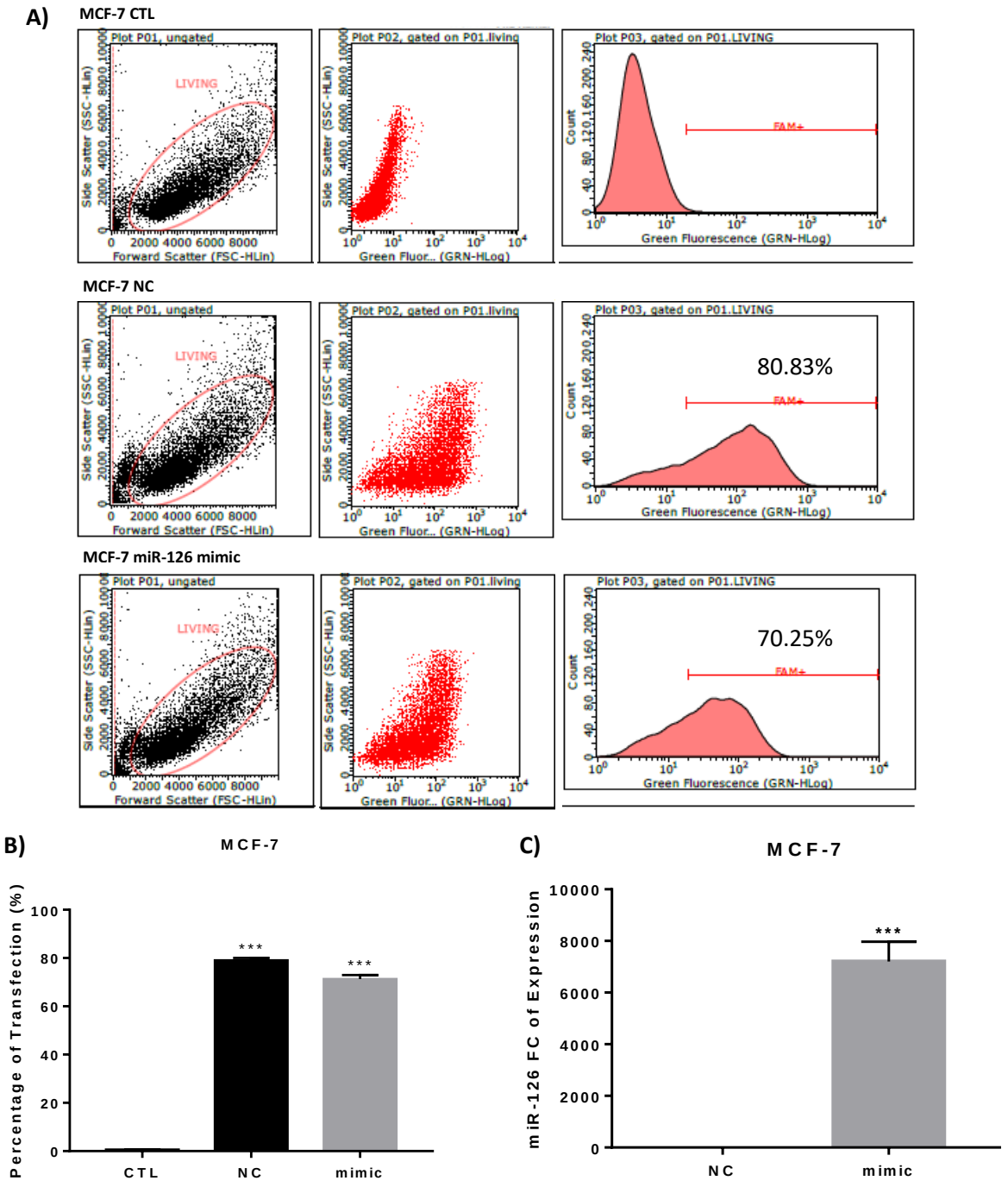

Figure 9. Transfection Efficiency of miR-126 mimic in MCF-7. Transfection efficiency was measured by flow cytometry and RT-qPCR in MCF-7 24hrs post transfection. (A): Representative figures of flow cytometric analysis of miR-126 mimic and NC transfected cells as compared to CTL, (B): Percentage of miR-126 mimic and NC transfected cells as compared to CTL, (C): RT-qPCR analysis of miR-126 levels as compared to NC, RNU6B was used as an endogenous control. Error bars represent SEM (n=3). *** $p<0.001$.

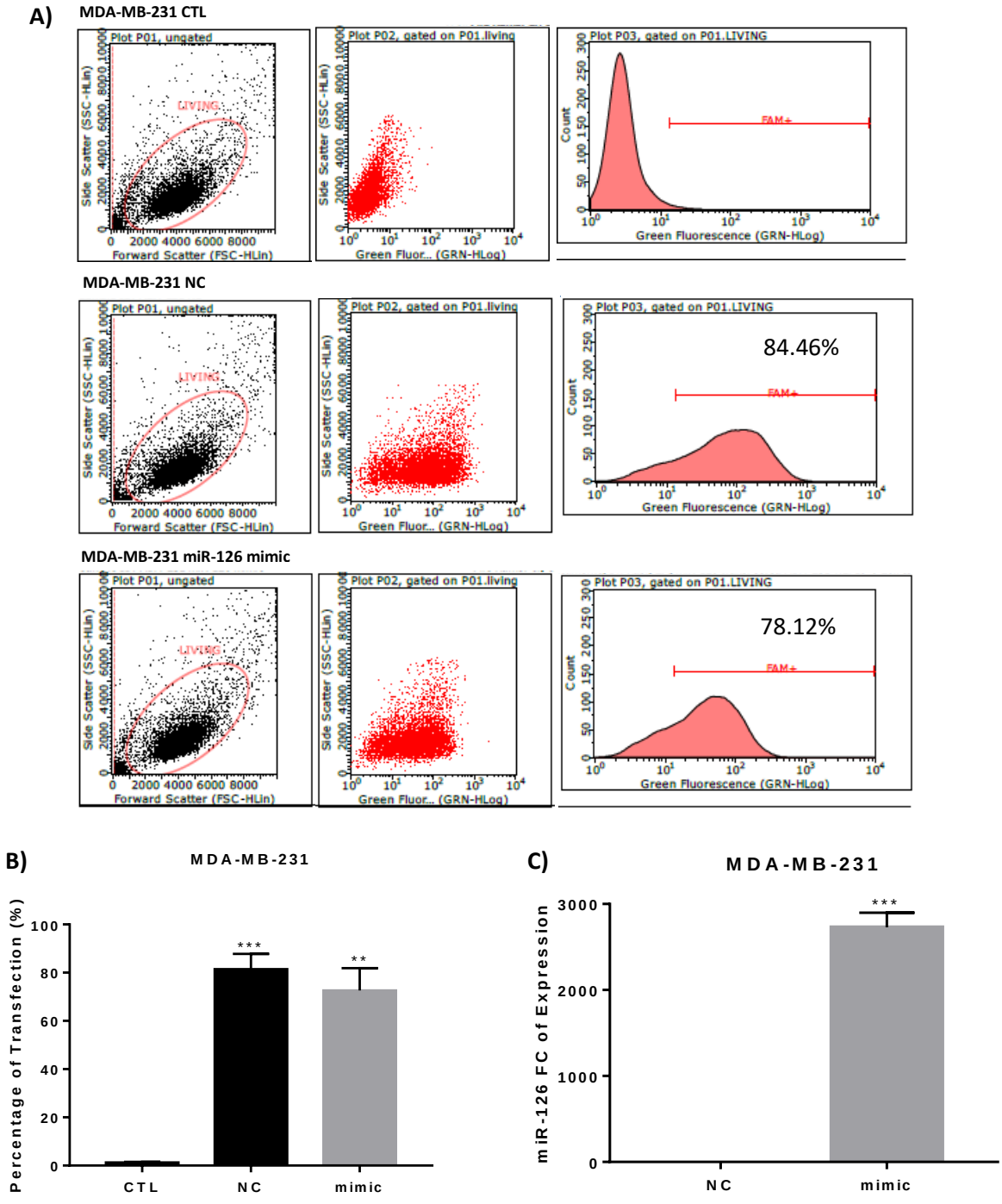

Figure 10. Transfection Efficiency of miR-126 mimic in MDA-MB-231. Transfection efficiency was measured by flow cytometry and RT-qPCR in MDA-MB-231 24hrs post transfection. (A): Representative figures of flow cytometric analysis of miR-126 mimic and NC transfected cells as compared to CTL, (B): Percentage of miR-126 mimic and NC transfected cells as compared to CTL, (C): RT-qPCR analysis of miR-126 levels as compared to NC, RNU6B was used as an endogenous control. Error bars represent SEM (n=4). ** denotes $p<0.01$, *** denotes $p<0.001$.

4. miR-126 inhibits MCF-7 cell proliferation and has no effect on proliferation of MCF-10A and MDA-MB-231

To determine the effect of miR-126 overexpression on proliferation of MCF-10A, MCF-7, and MDA-MB-231, MTT was done. There was no significant difference in the proliferation of miR-126 mimic transfected MCF-10A and MDA-MB-231 cells when compared to NC duplex transfected cells at 24, 48, and 72 hours. However, miR-126 significantly decreased the proliferation of MCF-7 72hrs post transfection ($p=0.034$) (Figure 11). This indicates that miR-126 has no effect on cell proliferation of MCF-10A and MDA-MB-231 and only reduces proliferation of MCF-7 72hrs post transfection.

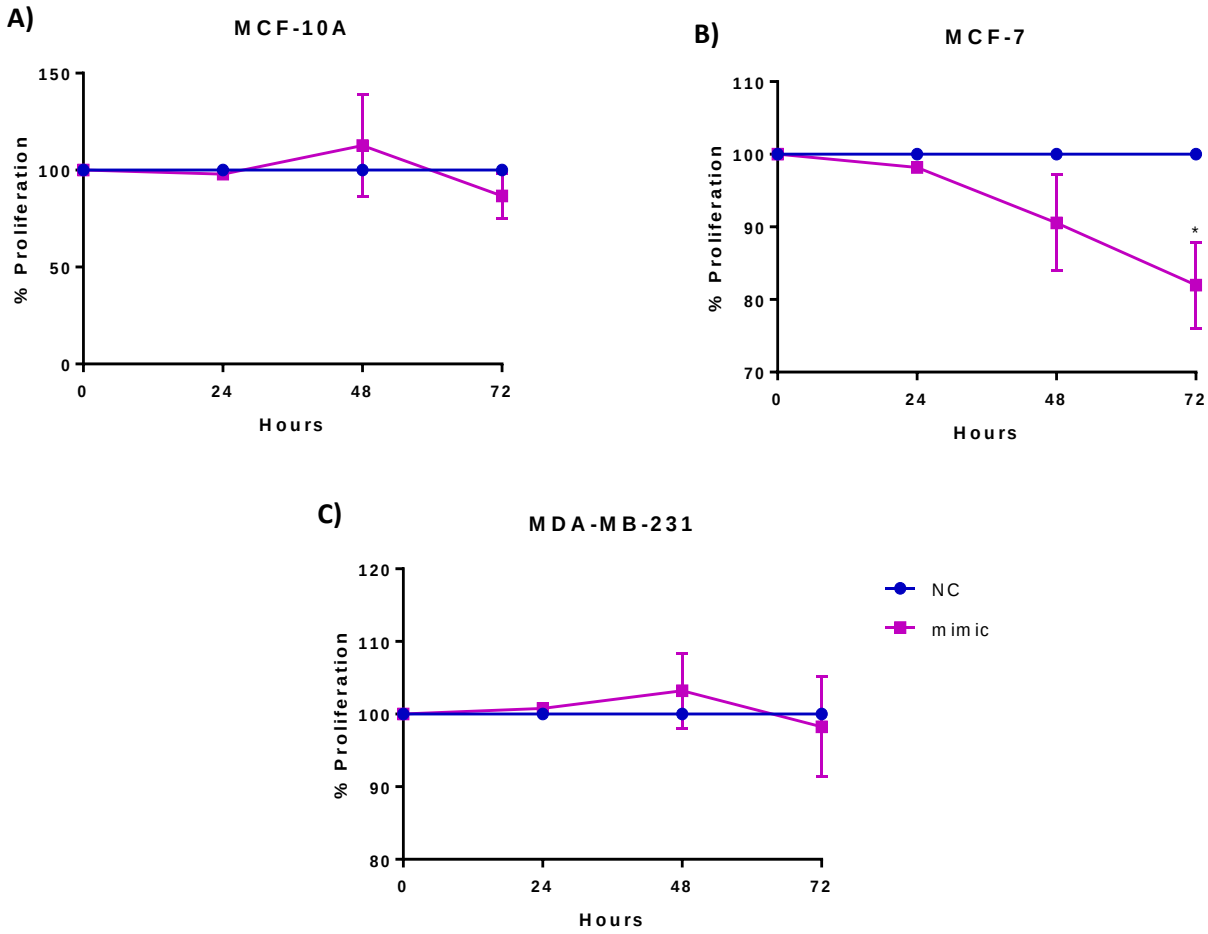

Figure 11. Proliferation of miR-126 mimic compared to NC transfected cells by MTT assay at 24, 48, and 72hrs post transfection. (A): MCF-10A, (B): MDA-MB-231, (C): MCF-7. Error bars represent SEM. 24hrs (n=1), 48 and 72hrs (n=3). * denotes $p<0.05$.

5. miR-126 has no effect on cell cycle progression of MCF-10A, MCF-7, and MDA-MB-231

To determine the effect of miR-126 on the cell cycle of MCF-10A, MCF-7, and MDA-MB-231, PI assay was done. There was no difference in the cell cycle phases of miR-126 mimic transfected cells when compared to NC duplex transfected cells 24 or 48 hours post transfection (Figures 12-14). This indicates that miR-126 has no effect on the cell cycle progression of the selected cell line.

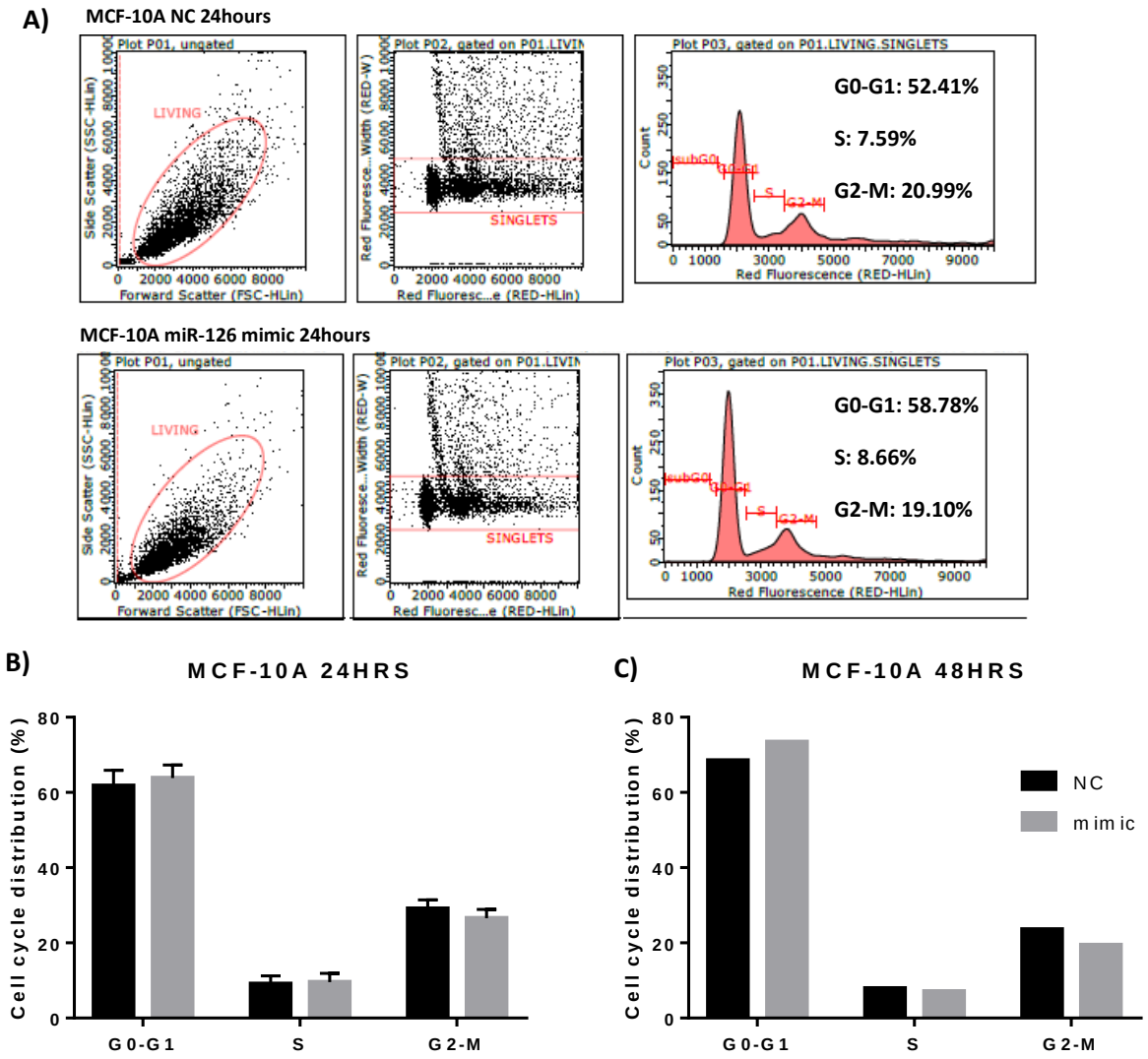

Figure 12. Cell Cycle Analysis of miR-126 mimic compared to NC MCF-10A transfected cells by PI staining. (A): Representative figures of flow cytometric analysis of the cell cycle in MCF-10A 24hrs post transfection, (B): Percentage of cells in each cell cycle phase 24hrs post transfection (n=3), (C): Percentage of cells in each cell cycle phase 48hrs post transfection (n=1). Error bars represent SEM.

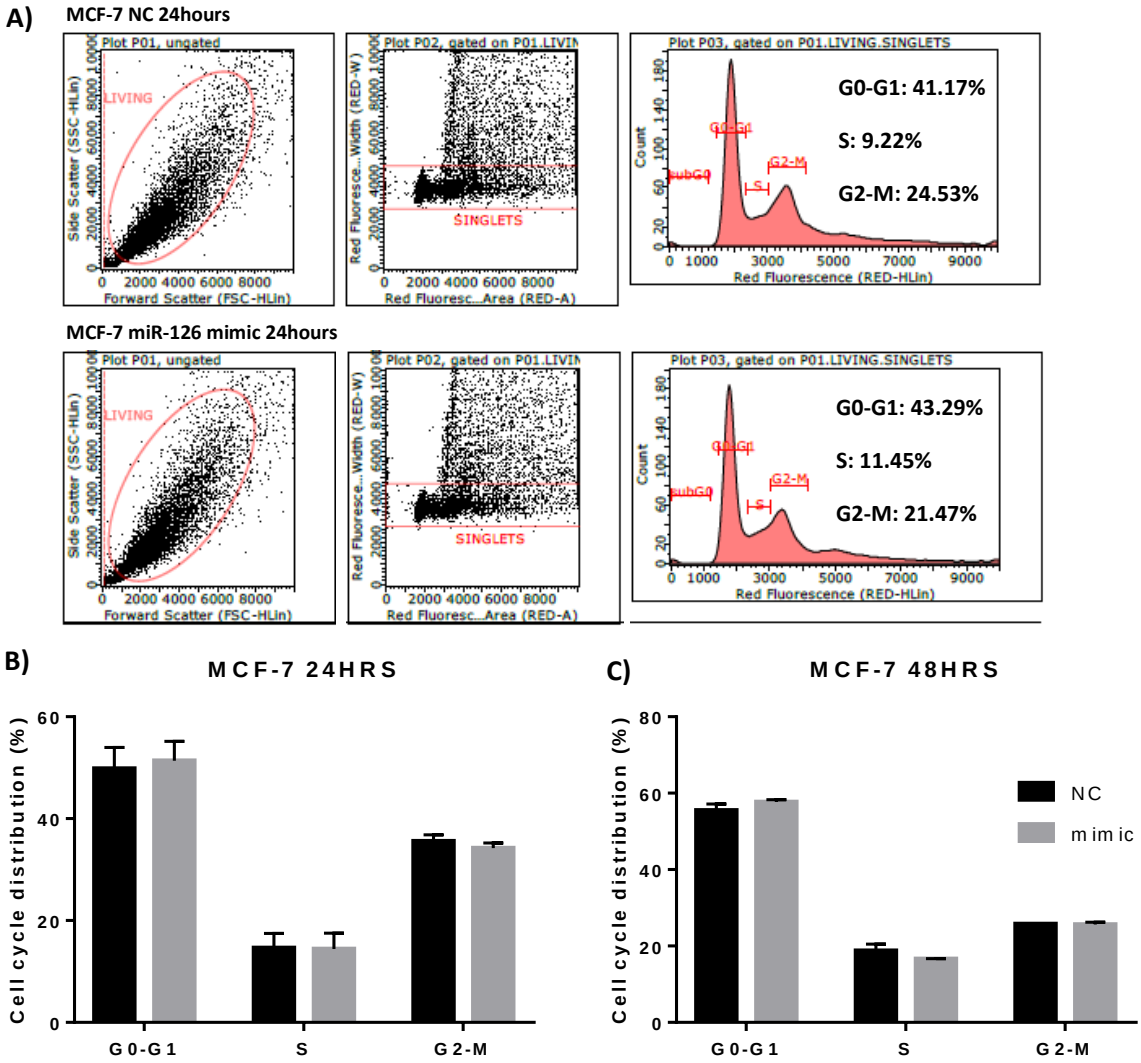

Figure 13. Cell Cycle Analysis of miR-126 mimic compared to NC MCF-7 transfected cells by PI staining. (A): Representative figures of flow cytometric analysis of the cell cycle in MCF-7 24hrs post transfection, (B): Percentage of cells in each cell cycle phase 24hrs post transfection (n=3), (C): Percentage of cells in each cell cycle phase 48hrs post transfection (n=2). Error bars represent SEM.

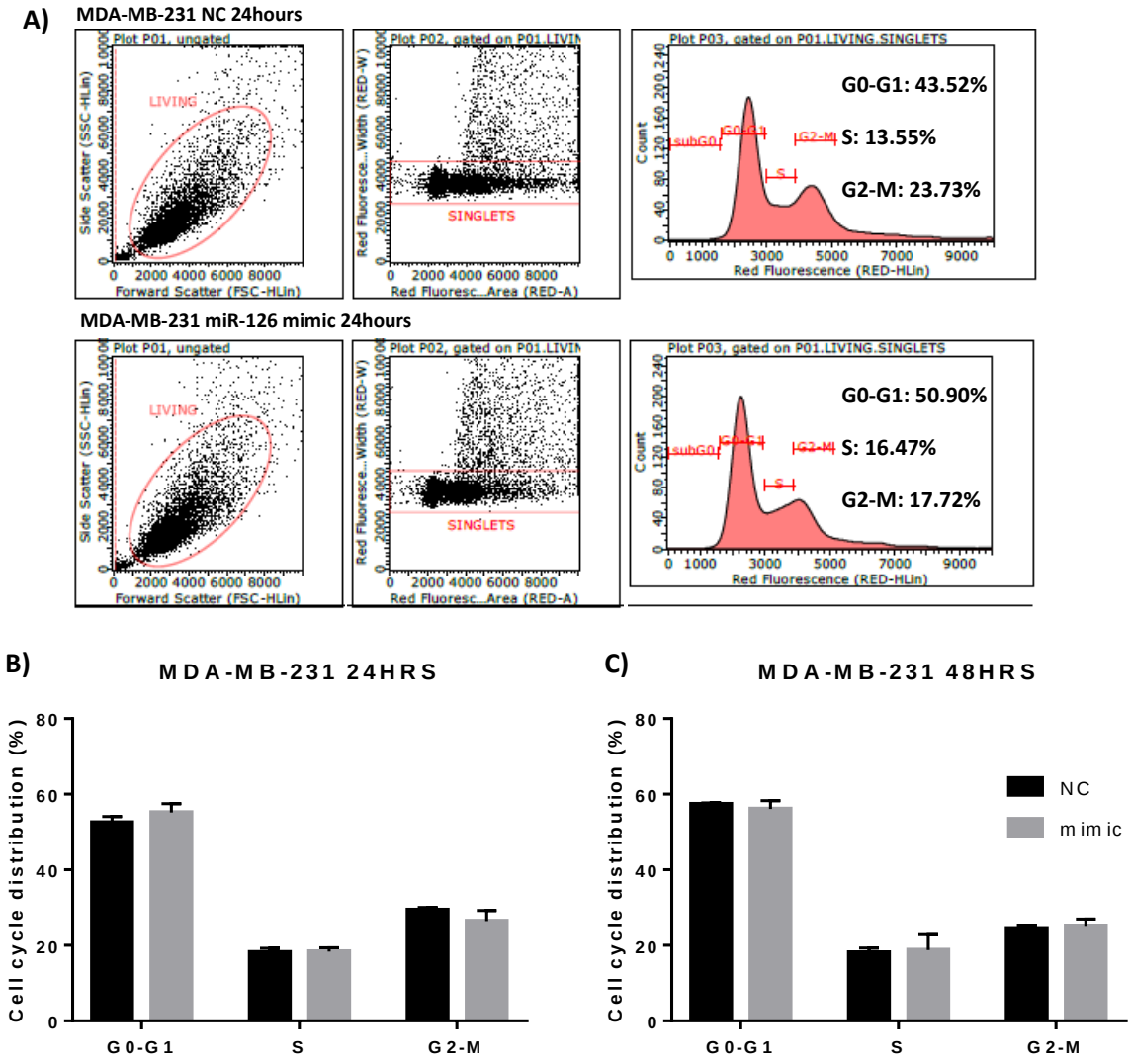

Figure 14. Cell Cycle Analysis of miR-126 mimic compared to NC MDA-MB-231 transfected cells by PI staining. (A): Representative figure of flow cytometric analysis of the cell cycle in MDA-MB-231 24hrs post transfection, (B): Percentage of cells in each cell cycle phase 24hrs post transfection (n=3), (C): Percentage of cells in each cell cycle phase 48hrs post transfection (n=2). Error bars represent SEM.

6. Effect of miR-126 on Mammospheres Formation of MCF-7 and MDA-MB-231

To determine the effect of miR-126 on mammospheres formation of MCF-7 and MDA-MB-231, spheres assay was done (Figure 15A). Our results showed that there was a trend towards a decrease in the number of spheres formed in miR-126 transfected MCF-7 and MDA-MB-231 when compared to NC transfected cells in both, primary and secondary generations. (Figure 15B, C).

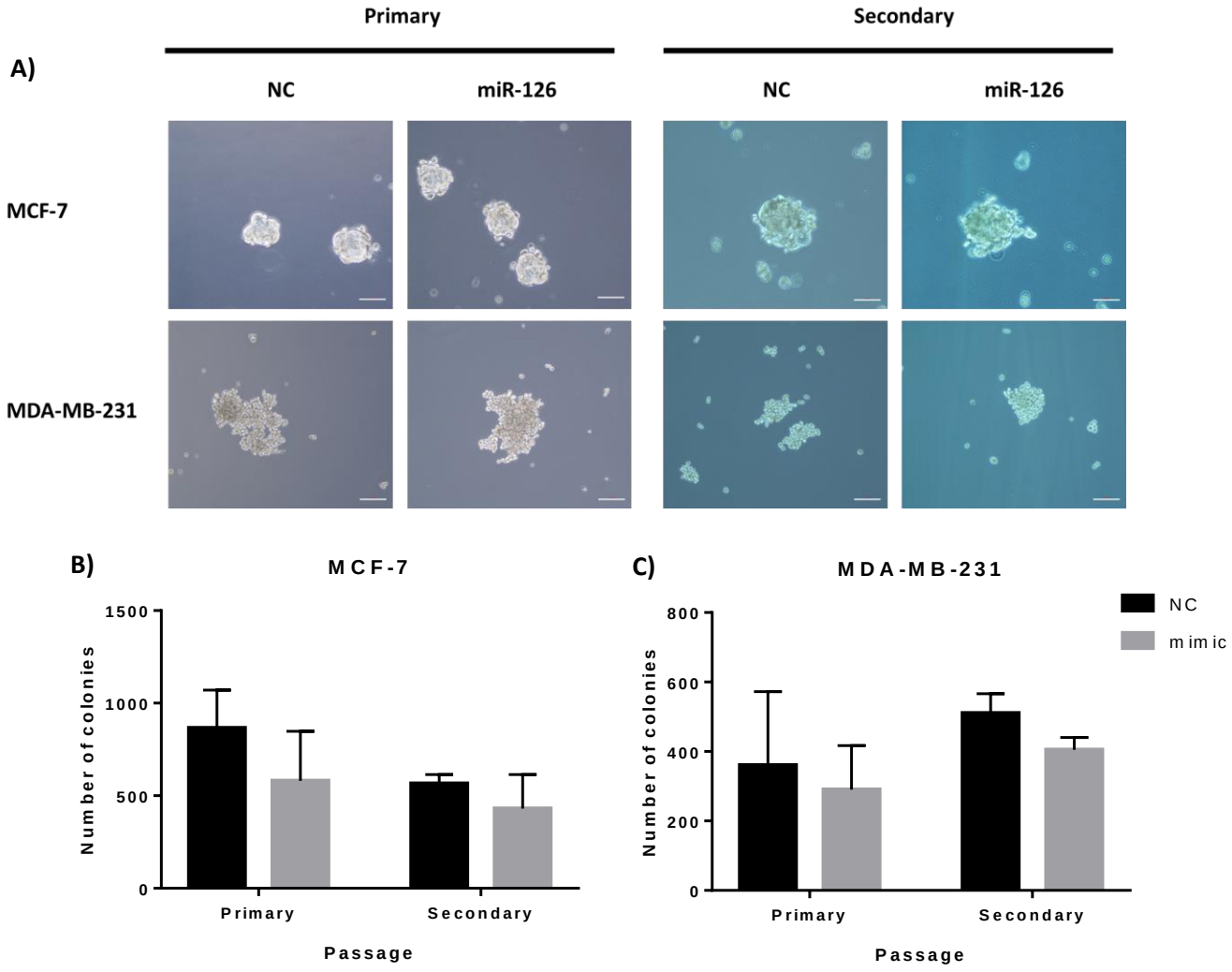

Figure 15. Mammospheres Forming Ability of miR-126 mimic compared to NC transfected BC cells. (A): Representative images of mammospheres formed from NC and miR-126 transfected MCF-7 and MDA-MB-231. Scale bar: 100µm. (B): Number of spheres/colonies in MCF-7, (C): Number of spheres/colonies in MDA-MB-231. Error bars represent SEM (n=2).

7. Selection of Predicted and Experimentally Validated mRNA Targets of miR-126

miR-126 targets were selected through two predicted target databases microT-CDS and TargetScanHuman 7.2, and an experimentally validated database Tarbase 7.0. PubMed search was performed to rule out miRNA-mRNA interactions validated in BC and to check for validated miRNA-mRNA interaction in other types of cancer, in addition, to check for the role of the resulting mRNA targets in BC in particular and in all types of cancer in general (Figure 16). As such, the following targets were selected: PLXNB2, SLC7A5, SPRED1, PLK2, HOXA9, MMP7, CRK, and IRS1 (Table 8).

Table 8. Selection Criteria of miR-126 Potential mRNA Targets in BC

Target	Name	microT-CDS	TargetScan	Tarbase	Validated relation of miRNA with BC	Validated relation of miRNA with other cancers
PLXNB2	plexin B2	Yes	Yes	No	No	Yes
SLC7A5 (LAT1)	solute carrier family 7 member 5	Yes	Yes	Yes	No	Yes
SPRED1	sprouty-related EVH1 domain containing 1	Yes	Yes	No	No	Yes
PLK2	polo-like kinase 2	Yes	Yes	No	No	Yes
HOXA9	homeobox A9	No	No	Yes	No	Yes
MMP7	metalloprotease 7	No	No	Yes	No	Yes
CRK	CRK proto-oncogene, adaptor protein	No	Yes	No	No	Yes
IRS1	insulin receptor substrate 1	Yes	Yes	No	Yes	Yes

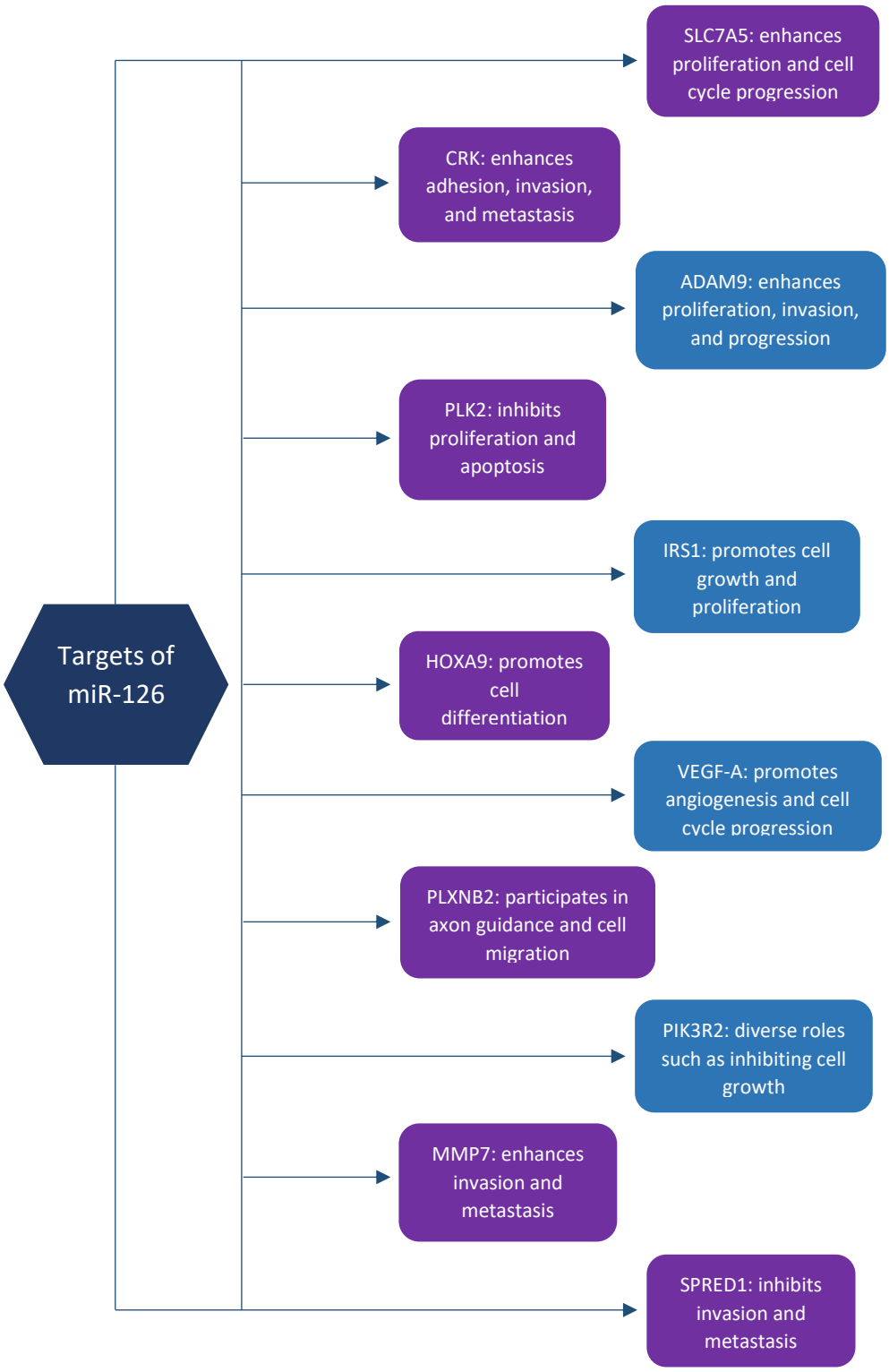

Figure 16. Functions of the Selected miR-126 Validated Targets in Cancer. Blue color indicates miR-126_mRNA validated relation in breast cancer. Purple color indicates miR-126_mRNA validated relation in other types of cancer. The latter will be further explored in our study.

8. Optimization of the Annealing Temperature and the Concentration of the Primers

Primers of the selected target genes were designed on PrimerBank and checked on PrimerBlast. The respective sequences and melting temperatures of the primers, in addition to the lengths of the products are shown in Table 9.

The annealing temperature and the concentration of the primers of the selected target genes were optimized in MCF-7 by RT-qPCR. Analysis showed that all target genes functioned at 60ºC except for MMP7 and HOXA9. 200nM was the optimal concentration for SLC7A5, PLXNB2, CRK, and PLK2, 400nM for SPRED1, and 500nM for IRS1 (Figure 17). The concentration and temperature of GAPDH are 500nM and 60ºC, respectively. MMP7 and HOXA9 primers were tried on a temperature gradient but, they did not function.

Table 9. Sequence and Melting Temperature (Tm) of Primers of GAPDH and miR-126 Predicted Targets designed on PrimerBank.

Gene	Primer	Sequence	Tm (ºC)	Product Size
GAPDH	GAPDH-F	5'-ACAACTTTGGTATCGTGGAAGG-3'	60.2	101
	GAPDH-R	5'-GCCATCACGCCACAGTTTC-3'	61.7	
PLXNB2	PLXNB2-F	5'-AGCCTCTTCAAGGGCATCTG-3'	61.6	95
	PLXNB2-R	5'-GCCACGAAAGACTTCTCCCC-3'	62.5	
SLC7A5	SLC7A5-F	5'-GGAAGGGTGATGTGTCCAATC-3'	60.4	83
	SLC7A5-R	5'-TAATGCCAGCACAATGTTCCC-3'	60.9	
SPRED1	SPRED1-F	5'-CAGCCAGGCTTGGACATTCA-3'	62.5	83
	SPRED1-R	5'-TGGGACTTTAGGCTTCCACAT-3'	60.8	
PLK2	PLK2-F	5'-CTACGCCGCAAAAATTATTCCTC-3'	60.2	138
	PLK2-R	5'-TCTTTGTCCTCGAAGTAGTGGT-3'	60.4	
HOXA9	HOXA9-F	5'-GTCCAAGGCGACGGTGTTT-3'	62.8	245
	HOXA9-R	5'-CCGACAGCGGTTCAGGTTTA-3'	62.1	
MMP7	MMP7-F	5'-GAGTGAGCTACAGTGGGAACA-3'	61.6	158
	MMP7-R	5'-CTATGACGCGGGAGTTTAACAT-3'	60.2	
CRK	CRK-F	5'-GGAGACATCTTGAGAATCCGGG-3'	61.9	95
	CRK-R	5'-ACGTAAGGGACTGGAATCATCC-3'	61.2	
IRS1	IRS1-F	5'-CCCAGGACCCGCATTCAAA-3'	62.3	89
	IRS1-R	5'-GGCGGTAGATACCAATCAGGT-3'	61.1	

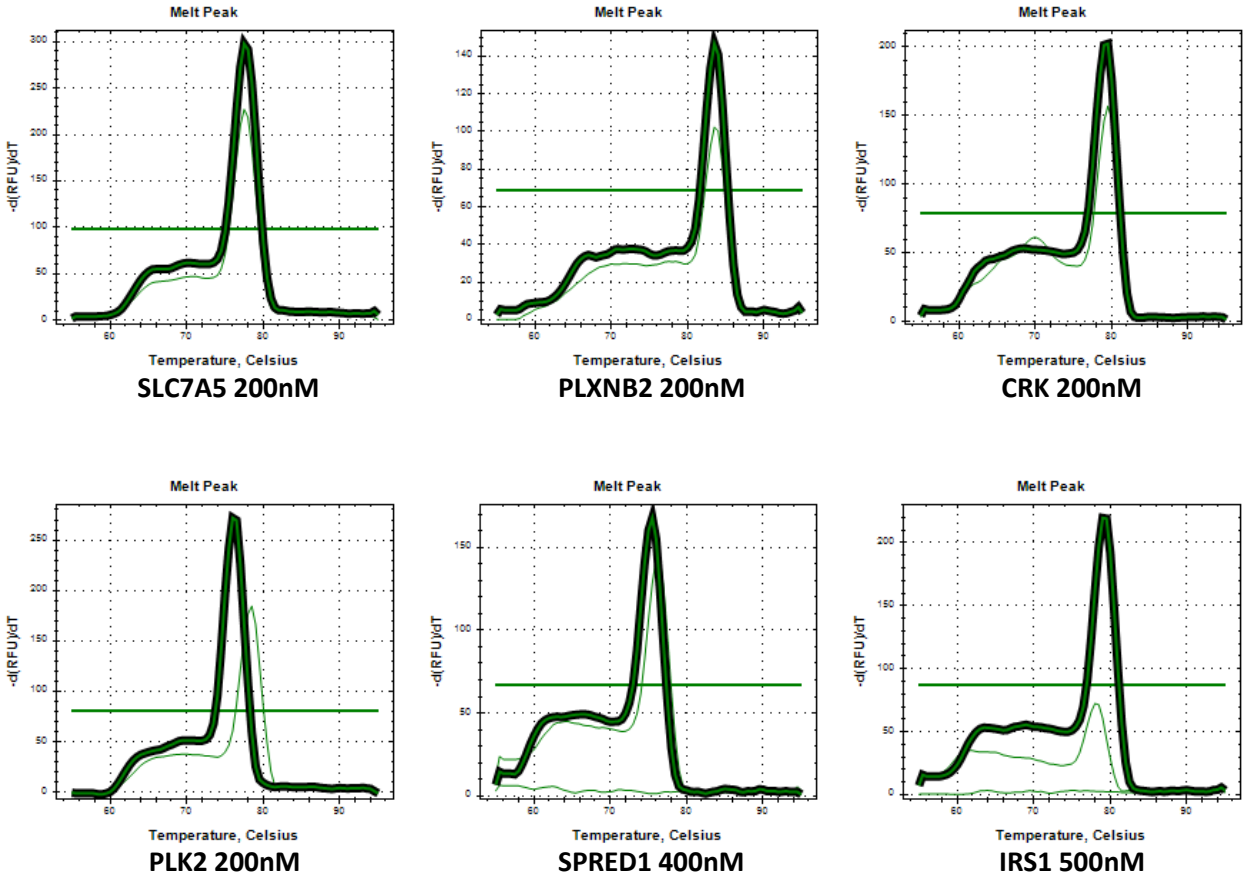

Figure 17. Melting Peaks of the Optimized Target Genes Primers. SLC7A5, PLXNB2, CRK, PLK2, SPRED1, and IRS1 were optimized at 60ºC with 200nM being the optimal concentration for SLC7A5, PLXNB2, CRK, and PLK2, 400nM for SPRED1, and 500nM for IRS1.

9. miR-126 targets mRNA of SLC7A5 and PLXNB2

To explore whether miR-126 targets SLC7A5, PLXNB2, CRK, PLK2, SPRED1, and IRS1, RT-qPCR was done on miR-126 mimic transfected cells as compared to NC duplex transfected cells 24 hours post transfection with GAPDH used as an internal control. mRNA of SLC7A5 was significantly downregulated in MCF-7 and MDA-MB-231 but not in MCF-10A and PLXNB2 was significantly downregulated in MCF-7 but not in MDA-MB-231 or MCF-10A. On the other hand, mRNA of PLK2, CRK, SPRED1, and IRS1 did not show any significant change in expression in all cell lines (Figure 18).

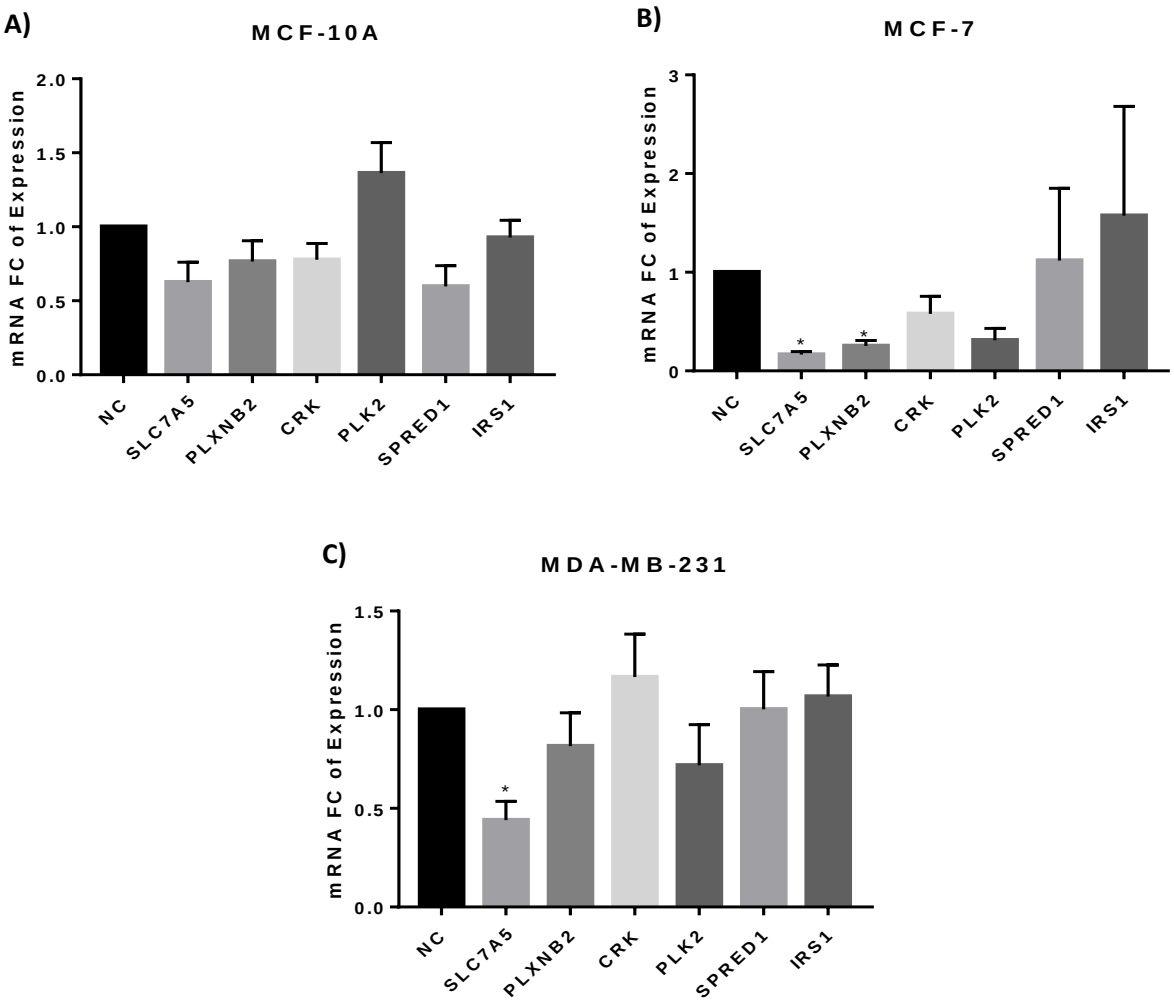

Figure 18. Expression Levels of Potential miR-126 Targets in miR-126 mimic compared to NC transfected cells 24hrs post transfection by RT-qPCR. (A): MCF-10A, (B): MCF-7, (C): MDA-MB-231. GAPDH was used as an internal control. Error bars represent SEM (n=3 for MCF-10A and MCF-7, n=4 for MDA-MB-231). * denotes $p<0.05$

10. High Expression of miR-126 or Low Expression of SLC7A5 correlates with better survival in ER+ BC patients

To determine if miR-126 or SLC7A5 expression could predict prognosis, *in silico* Kaplan-Meier analysis was done. We selected SLC7A5 for further analysis since it was the only significantly dysregulated target in the two BC cell lines, MCF-7 and MDA-MB-231. ER+ patients were selected since our clinical samples expressed estrogen receptor. In

addition, METABRIC database was selected since it includes patients with long-term follow-up. A total of 966 ER+ patients were obtained for miR-126 expression and a total of 548 ER+ patients were obtained for SLC7A5 expression. It was found that the overall survival significantly increased with high expression of miR-126 or with low expression of SLC7A5. Conversely, low expression of miR-126 or high expression of SLC7A5 were significantly associated with poor survival ($p=0.00014$ and $p=4.4\times10^{-6}$, respectively) (Figure 19). This shows the potential role of miR-126 and SLC7A5 as prognostic biomarkers in ER+ BC patients.

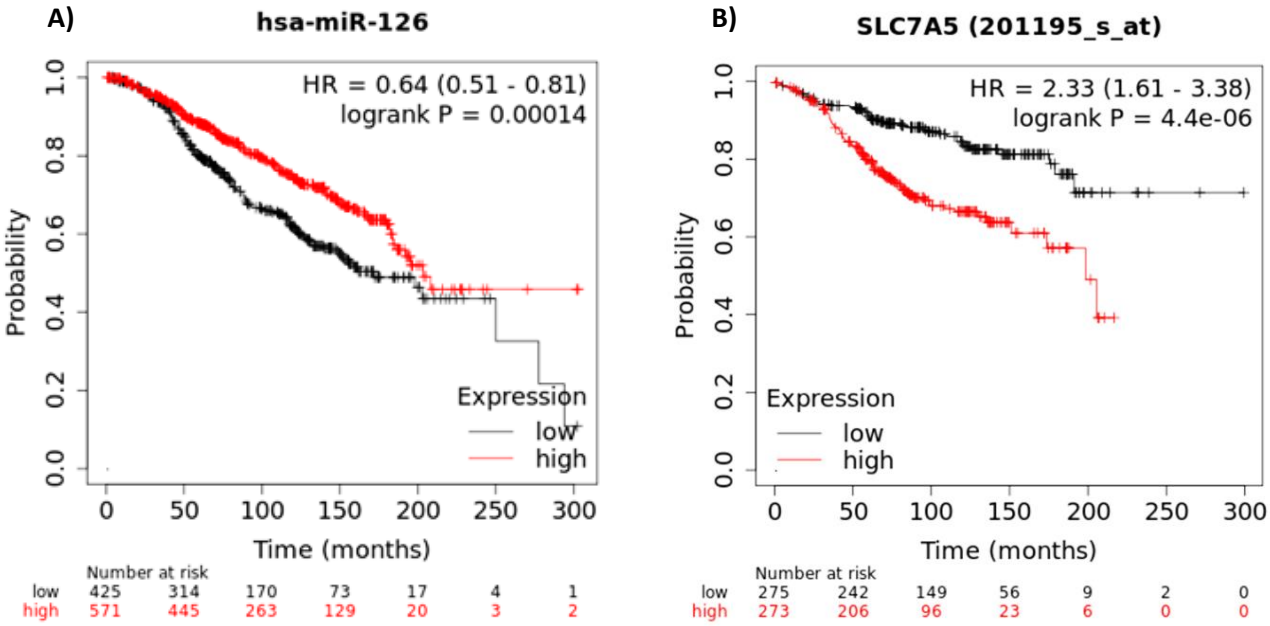

Figure 19. *In Silico* KM Plot showing the correlation between the Expression of miR-126 or SLC7A5 and Overall Survival (OS) in ER+ BC Patients. (A): Correlation of miR-126 expression with OS, (B): Correlation of SLC7A5 expression with OS. HR: Hazard Ratio

CHAPTER IV

DISCUSSION

Breast cancer is the deadliest type of cancer in women worldwide and in Lebanon. Although genetic predispositions, particularly mutations in *BRCA1* and *BRCA2*, are important drivers of this malignancy, epigenetic alterations may play an important role in the development of this disease [21]. Over the past several years, miRNAs were found to play diverse roles in various types of cancer including breast cancer. In addition, miRNAs were reported as potential biomarkers and might serve as potential diagnostic, prognostic, and therapeutic targets [70]. Several oncogenic or tumor suppressor miRNAs have been shown to play diverse roles in the different cellular pathways of breast cancer development such as cell proliferation, apoptosis, metastasis, and therapy resistance [83]. Analysis of miRNA expression profiles in Lebanese BC patients revealed the dysregulation of several oncomiRs and tsmiRs in BC tissues as compared to normal adjacent ones. Of these miRNAs, miR-126 was significantly downregulated [106]. miR-126 was reported to play diverse roles in different types of cancer including breast cancer (Table 3). Hence, this stimulated our interest to further understand its role in breast cancer development which may ultimately serve as a therapeutic target.

First, our group validated the downregulation of miR-126 revealed by the microarray analysis in Lebanese BC tissues by RT-qPCR. This is in accordance with the literature that reported the downregulation of miR-126 in BC tissues compared to normal adjacent ones from patients of different ethnicities (e.g. Chinese, Egyptian, Iranian) [113,

114, 117, 119]. This shows that miR-126 might play a tumor suppressor role in breast cancer.

Then, we checked for the expression of miR-126 in MCF-7 and MDA-MB-231 BC cell lines compared to the non-tumorigenic epithelial cell line MCF-10A. Our results showed that miR-126 is significantly upregulated in MCF-7 and MDA-MB-231 as compared to MCF-10A. However, this is in contrast to the literature, where it was shown that miR-126 is downregulated in MDA-MB-231 when compared to MCF-10A [120] and in both MDA-MB-231 and MCF-7 when compared to HUVEC [121]. Importantly, a study conducted in 2015 questioned the use of MCF-10A as a normal mammary epithelial cell line. They showed that MCF-10A expressed basal, luminal, and stem-like markers in 2D culture and exhibited a unique epithelial cell marker in 3D culture that was not observed previously in mammary gland tissues. Therefore, further studies are needed to confirm the use of MCF-10A as a normal epithelial cell lines [122].

Although our results have shown that miR-126 was upregulated in MCF-7 and MDA-MB-231 as compared to MCF-10A, however, this study was conducted first based on the literature that reported the downregulation of miR-126 in the BC cell lines. Thus, miR-126 was overexpressed by transfection with miR-126 mimic. Flow cytometric analysis showed that transfection with miR-126 mimic and NC was successfully done in the MCF-10A, MCF-7, and MDA-MB-231. Analysis of miR-126 levels by RT-qPCR showed that miR-126 was certainly overexpressed upon transfection with the mimic. Although miR-126 was significantly overexpressed, an inhibition in cell proliferation was only seen in MCF-7 cells, mild decrease in mammospheres formation in MCF-7 and MDA-

MB-231, and no effect on cell cycle progression in all 3 cell lines. To our knowledge, this is the first time MCF-10A is tested for the overexpression of miR-126.

Multiple studies showed that miR-126 overexpression decreased cell proliferation of MCF-7 and MDA-MB-231 [115, 120, 121, 123-125] whereas others showed that it had no effect on the proliferation of these cell lines [116]. miR-126 overexpression also decreased the proliferation of HCC1937 (TN) [120], while it had no effect on the proliferation of MCF10ADCIS (DCIS derived) [113]. In addition, miR-126 inhibition increased cell proliferation of MCF-7 and MDA-MB-231 upon transfection with miR-126 inhibitor [120, 124]. Different methods were utilized to determine the effect of miR-126 on the proliferation of these cell lines. These include MTT, MTS, XTT, CCK-8, RTCA, and Picogreen assays. Our results using MTT did not reveal any effect of miR-126 on the proliferation of MCF-10A and MDA-MB-231 and only showed significant decrease in the proliferation of MCF-7 72 hours post transfection. Moreover, our data showed that miR-126 had no effect on the cell cycle progression of all tested cell lines. However, two studies reported that miR-126 inhibited G0-G1 to S phase transition in MCF-7. These were done 24 hours post transfection by DAPI and 60 hours post transfection by PI staining [121, 123]. As for mammospheres formation, ectopic expression of miR-126 resulted in a mild decrease in mammospheres formation ability but, without significant difference when compared with that exhibited by NC transfected cells. This is consistent with a recent study that reported that miR-126 overexpression inhibited MDA-MB-231 spheres formation ability [120]. However, an older study conducted in 2015 showed that miR-126 had no effect on the ability of MDA-MB-231 to form spheres [115], although same method of

colony formation and cell number was used in both studies. This contradiction in the reported results of miR-126 on cellular processes might be attributed to the different modes of transfection, the time points at which the assays were done, and the methods utilized. In addition, the difference in the BC cell lines responses to miR-126 might be explained by their hormone receptor expression profile and the molecular subtype they resemble. The mentioned effects of miR-126 on BC progression is shown to be mediated by different validated targets including IRS-1, VEGF-A, and RGS3 [120, 121, 123]. The respective timepoints (24 and 48 hours) were selected in our study based on previous data in our lab that showed that miR expression levels are the highest at 24 hours and decrease at later timepoints. It's noteworthy to mention that transfection with plasmids expressing miR-126 might show more promising results since it is a stable transfection.

Interestingly, we transfected the BC cell lines MCF-7 and MDA-MB-231 with miR-126 inhibitor, that decreases the levels of miR-126, to check whether it has the opposite effects of the mimic. Upon analyzing the expression levels of miR-126 in the transfected cells, it showed almost the same levels as in the NC transfected cells (data not shown). However, in such cases, the protein levels of the target genes might be dysregulated. As such, detecting the protein levels of the targets would give an insight on the active function of the inhibitor.

Then, we investigated the association of miR-126 and some potential targets that was determined by *in silico* analysis. Among miR-126 potential targets that we studied is IRS1 that plays a crucial role in cell growth mainly through the PI3/Akt pathway. Activation of IRS1 has been reported to occur in several types of cancers including breast

cancer. IRS1 was validated as a direct target of miR-126 in BC by luciferase vector assay. Interestingly, they did not find any effect of miR-126 overexpression on the mRNA levels while it decreased the protein levels. [121]. This is in accordance to our data that revealed no significant change in IRS1 mRNA expression levels upon transfection with miR-126 mimic. The expression of SPRED1, a key player in VEGF signal transduction pathway that plays an important role in angiogenesis, was also investigated in our study. *Cosan et al.* reported that miR-126 mimic nonsignificantly increased the mRNA levels of SPRED1 in BC which is consistent with our data [124]. They also showed that miR-126 inhibitor significantly increased SPRED1 mRNA levels. The inverse relation of PLK2 and CRK targets with miR-126 was not previously validated in BC nor they were in our study. Targets that were not dysregulated at the mRNA level may show significant dysregulation at the protein level. Hence, it would be interesting to check their protein levels.

Importantly, our data showed downregulation of the oncogenes SLC7A5 and PLXNB2 upon transfection with miR-126 mimic in BC cell lines. This is the first report of the inverse correlation between miR-126 and these targets in BC. Interestingly, mRNA microarray analysis done on the Lebanese BC tissues previously mentioned revealed the upregulation of SLC7A5 and PLXNB2 that reiterates the tumor suppressive role of miR-126 in suppressing these oncogenic targets.

PLXNB2 is a transmembrane receptor that participates in the development of the nervous system and cell migration. PLXNB2 is highly upregulated in human gliomas and its expression level correlates with tumor grade and poor survival. *Gurrapu et al.* showed that upon knockdown of PLXNB2 or its ligand semaphorin 4C in different BC cell lines,

growth was dramatically inhibited along with impairment of G2/M phase transition, cytokinesis defects, and cell senescence [126]. *Xiang et al.* showed that miR-126 overexpression decreased PLXNB2 mRNA and protein levels in ovarian cancer (OC). PLXNB2 knockdown repressed OC cell proliferation and invasion which was consistent with the results of miR-126 overexpression. In addition, they validated PLXNB2 as a direct target of miR-126 by luciferase reporter assay [127]. Similar to their results, we found that miR-126 overexpression in MCF-7 downregulated PLXNB2 mRNA levels.

SLC7A5 (or LAT1) is a sodium-independent amino acid transporter which is considered a master regulator of the mTORC1 signaling pathway. SLC7A5 is overexpressed in several types of cancer and was related to cancer progression and aggressiveness. A recent study revealed that high expression of SLC7A5 was associated with poor prognosis and poor survival outcome in the highly proliferative ER+ BC subtype (luminal B), indicating its role in the progression of the aggressive ER+ subtype and as a key therapeutic target [128]. Other studies showed high expression of SLC7A5 in HER2+ and TNBC subtypes. *Miko et al.* showed that miR-126 overexpression suppressed SLC7A5 mRNA and protein levels in small cell lung cancer cells (SCLC). Similar to miR-126 overexpression, SLC7A5 suppression resulted in increased percentage of cells in G0/G1 phase. Add to this, they validated the direct interaction between miR-126 and SLC7A5 by luciferase reporter assay [129]. Consistent with their results, we found that miR-126 overexpression in both BC cell lines, MCF-7 and MDA-MB-231, downregulated SLC7A5 mRNA levels. Considering the prognostic role of SLC7A5 in BC and the downregulation

of the mRNA levels in MCF-7 and MDA-MB-231 upon transfection with miR-126 mimic, we are interested in exploring its role further in BC in association with miR-126.

Finally, KM analysis was done to determine the association between the expression levels of miR-126 or SLC7A5 with the overall survival of ER+ BC patients. High expression levels of miR-126 or low expression levels of SLC7A5 were associated with better OS validating their role as potential prognostic biomarkers in BC. We were interested in checking the correlation between the expression of both, miR-126 and SLC7A5, concomitantly, and overall survival of BC patients, but this was not an available option in the *in silico* tool.

In conclusion, our study suggests that miR-126 might play a tumor suppressor role in breast cancer. miR-126 was downregulated in Lebanese breast cancer tissues and reduced the mRNA expression levels of SLC7A5, that was upregulated in the tissues as revealed by the microarray analysis, in both BC cell lines and PLXNB2 in only one cell line. Hence, as future perspectives, we will check the expression levels of SLC7A5 in the Lebanese BC tissues, we will also detect the protein expression levels of SLC7A5 in the transfected cell lines then, validate its direct interaction with miR-126 in the BC cell lines. We will also perform more functional assays to better understand the role of miR-126 and SLC7A5 in BC (Figure 20). Finally, this study helps shed light on the prognostic role of this studied microRNA and its potential target in breast cancer that will need further validation in more clinical samples.

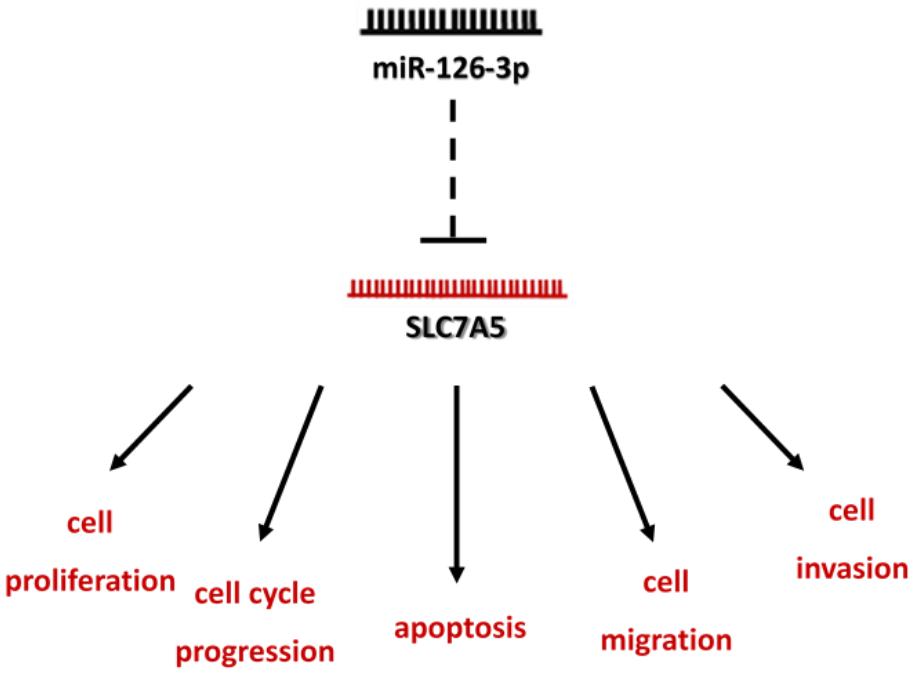

Figure 20. Summary of the Potential Role of miR-126 mediated through SLC7A5.

BIBLIOGRAPHY

1. Bray, F., et al., *Global cancer statistics 2018: GLOBOCAN estimates of incidence and mortality worldwide for 36 cancers in 185 countries.* CA Cancer J Clin, 2018. **68**(6): p. 394-424.
2. Fan, L., P.E. Goss, and K. Strasser-Weippl, *Current Status and Future Projections of Breast Cancer in Asia.* Breast Care (Basel), 2015. **10**(6): p. 372-8.
3. Tfayli, A., et al., *Breast cancer in low- and middle-income countries: an emerging and challenging epidemic.* J Oncol, 2010. **2010**: p. 490631.
4. Fares, M.Y., et al., *Breast Cancer Epidemiology among Lebanese Women: An 11-Year Analysis.* Medicina (Kaunas), 2019. **55**(8).
5. Lakkis, N.A., et al., *Breast cancer in Lebanon: incidence and comparison to regional and Western countries.* Cancer Epidemiol, 2010. **34**(3): p. 221-5.
6. Sibai, A.M., et al., *Prevalence and covariates of obesity in Lebanon: findings from the first epidemiological study.* Obesity research, 2003. **11**(11): p. 1353-1361.
7. Sadri, G. and H. Mahjub, *Passive or active smoking, which is more relevant to breast cancer.* Saudi medical journal, 2007. **28**(2): p. 254-258.
8. El Saghir, N.S., et al., *Trends in epidemiology and management of breast cancer in developing Arab countries: a literature and registry analysis.* Int J Surg, 2007. **5**(4): p. 225-33.
9. Assi, H.A., et al., *Epidemiology and prognosis of breast cancer in young women.* J Thorac Dis, 2013. **5 Suppl 1**: p. S2-8.
10. El Saghir, N.S., et al., *Effects of young age at presentation on survival in breast cancer.* BMC Cancer, 2006. **6**: p. 194.
11. El Saghir, N.S., et al., *BRCA1 and BRCA2 mutations in ethnic Lebanese Arab women with high hereditary risk breast cancer.* Oncologist, 2015. **20**(4): p. 357-64.
12. Farra, C., et al., *BRCA mutation screening and patterns among high-risk Lebanese subjects.* Hered Cancer Clin Pract, 2019. **17**: p. 4.
13. Pandya, S. and R.G. Moore, *Breast development and anatomy.* Clinical obstetrics and gynecology, 2011. **54**(1): p. 91-95.
14. Javed, A. and A. Lteif, *Development of the human breast.* Semin Plast Surg, 2013. **27**(1): p. 5-12.
15. Neville, M.C., *Anatomy and physiology of lactation.* Pediatric Clinics of North America, 2001. **48**(1): p. 13-34.
16. Macias, H. and L. Hinck, *Mammary gland development.* Wiley Interdiscip Rev Dev Biol, 2012. **1**(4): p. 533-57.
17. Albernaz, C., *Breast cancer: carcinogenesis, diagnosis and treatment.* EUR. J. ONCOL., 2017. **22**(2): p. 53-64.
18. Dumont, N., et al., *Breast fibroblasts modulate early dissemination, tumorigenesis, and metastasis through alteration of extracellular matrix characteristics.* Neoplasia, 2013. **15**(3): p. 249-62.
19. Lin, E.Y. and J.W. Pollard, *Tumor-associated macrophages press the angiogenic switch in breast cancer.* Cancer Res, 2007. **67**(11): p. 5064-6.

20. Allinen, M., et al., *Molecular characterization of the tumor microenvironment in breast cancer.* Cancer Cell, 2004. **6**(1): p. 17-32.
21. Polyak, K., *Breast cancer: origins and evolution.* J Clin Invest, 2007. **117**(11): p. 3155-63.
22. Beckmann, M., et al., *Multistep carcinogenesis of breast cancer and tumour heterogeneity.* Journal of molecular medicine, 1997. **75**(6): p. 429-439.
23. Turashvili, G. and E. Brogi, *Tumor heterogeneity in breast cancer.* Frontiers in medicine, 2017. **4**: p. 227.
24. Bertos, N.R. and M. Park, *Breast cancer - one term, many entities?* J Clin Invest, 2011. **121**(10): p. 3789-96.
25. Makki, J., *Diversity of Breast Carcinoma: Histological Subtypes and Clinical Relevance.* Clin Med Insights Pathol, 2015. **8**: p. 23-31.
26. Fu, D., et al., *Molecular classification of lobular carcinoma of the breast.* Scientific reports, 2017. **7**(1): p. 1-13.
27. Pećina-Šlaus, N., *Tumor suppressor gene E-cadherin and its role in normal and malignant cells.* Cancer cell international, 2003. **3**(1): p. 17.
28. Vuong, D., et al., *Molecular classification of breast cancer.* Virchows Arch, 2014. **465**(1): p. 1-14.
29. Bardou, V.-J., et al., *Progesterone receptor status significantly improves outcome prediction over estrogen receptor status alone for adjuvant endocrine therapy in two large breast cancer databases.* Journal of clinical oncology, 2003. **21**(10): p. 1973-1979.
30. Anderson, W.F., et al., *Estrogen receptor breast cancer phenotypes in the Surveillance, Epidemiology, and End Results database.* Breast cancer research and treatment, 2002. **76**(1): p. 27-36.
31. Patel, R.R., C.G. Sharma, and V.C. Jordan, *Optimizing the antihormonal treatment and prevention of breast cancer.* Breast cancer, 2007. **14**(2): p. 113-122.
32. Lumachi, F., D.A. Santeufemia, and S.M. Basso, *Current medical treatment of estrogen receptor-positive breast cancer.* World journal of biological chemistry, 2015. **6**(3): p. 231.
33. Liu, S., et al., *Progesterone receptor is a significant factor associated with clinical outcomes and effect of adjuvant tamoxifen therapy in breast cancer patients.* Breast cancer research and treatment, 2010. **119**(1): p. 53.
34. Arpino, G., et al., *Estrogen receptor–positive, progesterone receptor–negative breast cancer: association with growth factor receptor expression and tamoxifen resistance.* Journal of the National Cancer Institute, 2005. **97**(17): p. 1254-1261.
35. Dandachi, N., O. Dietze, and C. Hauser-Kronberger, *Chromogenic in situ hybridization: a novel approach to a practical and sensitive method for the detection of HER2 oncogene in archival human breast carcinoma.* Laboratory investigation, 2002. **82**(8): p. 1007-1014.
36. Junttila, T.T., et al., *Ligand-independent HER2/HER3/PI3K complex is disrupted by trastuzumab and is effectively inhibited by the PI3K inhibitor GDC-0941.* Cancer cell, 2009. **15**(5): p. 429-440.
37. Griffiths, C.L. and J.L. Olin, *Triple negative breast cancer: a brief review of its characteristics and treatment options.* Journal of pharmacy practice, 2012. **25**(3): p. 319-323.
38. Griffiths, C.L. and J.L. Olin, *Triple negative breast cancer: a brief review of its characteristics and treatment options.* J Pharm Pract, 2012. **25**(3): p. 319-23.
39. Xiao, G., et al., *Gain-of-Function Mutant p53 R273H Interacts with Replicating DNA and PARP1 in Breast Cancer.* Cancer research, 2020. **80**(3): p. 394-405.

40. O'Shaughnessy, J., et al., *Iniparib plus chemotherapy in metastatic triple-negative breast cancer.* New England Journal of Medicine, 2011. **364**(3): p. 205-214.
41. Group, E.B.C.T.C., *Tamoxifen for early breast cancer: an overview of the randomised trials.* The Lancet, 1998. **351**(9114): p. 1451-1467.
42. Smith, I., et al., *2-year follow-up of trastuzumab after adjuvant chemotherapy in HER2-positive breast cancer: a randomised controlled trial.* The lancet, 2007. **369**(9555): p. 29-36.
43. De Azambuja, E., et al., *Ki-67 as prognostic marker in early breast cancer: a meta-analysis of published studies involving 12 155 patients.* British journal of cancer, 2007. **96**(10): p. 1504-1513.
44. Perou, C.M., et al., *Molecular portraits of human breast tumours.* nature, 2000. **406**(6797): p. 747-752.
45. Sørlie, T., et al., *Gene expression patterns of breast carcinomas distinguish tumor subclasses with clinical implications.* Proceedings of the National Academy of Sciences, 2001. **98**(19): p. 10869-10874.
46. Sørlie, T., et al., *Repeated observation of breast tumor subtypes in independent gene expression data sets.* Proceedings of the national academy of sciences, 2003. **100**(14): p. 8418-8423.
47. Cheang, M.C., et al., *Ki67 index, HER2 status, and prognosis of patients with luminal B breast cancer.* JNCI: Journal of the National Cancer Institute, 2009. **101**(10): p. 736-750.
48. Prat, A., et al., *Phenotypic and molecular characterization of the claudin-low intrinsic subtype of breast cancer.* Breast cancer research, 2010. **12**(5): p. R68.
49. Blenkiron, C., et al., *MicroRNA expression profiling of human breast cancer identifies new markers of tumor subtype.* Genome biology, 2007. **8**(10): p. R214.
50. al., G.N.H.e., *Breast Cancer Staging System: AJCC Cancer Staging Manual, Eighth Edition.* Breast, 2017: p. 589-628.
51. Koh, J. and M.J. Kim, *Introduction of a New Staging System of Breast Cancer for Radiologists: An Emphasis on the Prognostic Stage.* Korean J Radiol, 2019. **20**(1): p. 69-82.
52. Schwartz, A.M., et al., *Histologic grade remains a prognostic factor for breast cancer regardless of the number of positive lymph nodes and tumor size: a study of 161 708 cases of breast cancer from the SEER Program.* Archives of Pathology and Laboratory Medicine, 2014. **138**(8): p. 1048-1052.
53. Elston, C.W. and I.O. Ellis, *Pathological prognostic factors in breast cancer. I. The value of histological grade in breast cancer: experience from a large study with long-term follow-up. CW Elston & IO Ellis. Histopathology 1991; 19; 403–410: AUTHOR COMMENTARY.* Histopathology, 2002. **41**(3a): p. 151-151.
54. Sparano, J.A., et al., *Prospective validation of a 21-gene expression assay in breast cancer.* New England Journal of Medicine, 2015. **373**(21): p. 2005-2014.
55. Van Gils, C.H., et al., *Effect of mammographic breast density on breast cancer screening performance: a study in Nijmegen, The Netherlands.* Journal of Epidemiology & Community Health, 1998. **52**(4): p. 267-271.
56. Checka, C.M., et al., *The relationship of mammographic density and age: implications for breast cancer screening.* American Journal of Roentgenology, 2012. **198**(3): p. W292-W295.

57. Burkett, B.J. and C.W. Hanemann, *A review of supplemental screening ultrasound for breast cancer: certain populations of women with dense breast tissue may benefit.* Academic radiology, 2016. **23**(12): p. 1604-1609.
58. Van Goethem, M., et al., *Magnetic resonance imaging in breast cancer.* European Journal of Surgical Oncology (EJSO), 2006. **32**(9): p. 901-910.
59. Palmer, M.L. and T.N. Tsangaris, *Breast biopsy in women 30 years old or less.* The American journal of surgery, 1993. **165**(6): p. 708-712.
60. Brooks, M., *Breast cancer screening and biomarkers*, in *Cancer Epidemiology*. 2009, Springer. p. 307-321.
61. Vieira, A.F. and F. Schmitt, *An update on breast cancer multigene prognostic tests—emergent clinical biomarkers.* Frontiers in medicine, 2018. **5**: p. 248.
62. Zhu, W., et al., *Circulating microRNAs in breast cancer and healthy subjects.* BMC research notes, 2009. **2**(1): p. 89.
63. Mayer, E.L., *Targeting breast cancer with CDK inhibitors.* Current oncology reports, 2015. **17**(5): p. 20.
64. Vinayak, S. and R.W. Carlson, *mTOR inhibitors in the treatment of breast cancer.* Breast Cancer, 2013. **27**(1).
65. Ha, M. and V.N. Kim, *Regulation of microRNA biogenesis.* Nature reviews Molecular cell biology, 2014. **15**(8): p. 509-524.
66. Lee, R.C., R.L. Feinbaum, and V. Ambros, *The C. elegans heterochronic gene lin-4 encodes small RNAs with antisense complementarity to lin-14.* cell, 1993. **75**(5): p. 843-854.
67. Pasquinelli, A.E., et al., *Conservation of the sequence and temporal expression of let-7 heterochronic regulatory RNA.* Nature, 2000. **408**(6808): p. 86-89.
68. Friedländer, M.R., et al., *Evidence for the biogenesis of more than 1,000 novel human microRNAs.* Genome biology, 2014. **15**(4): p. R57.
69. Lee, Y., et al., *MicroRNA maturation: stepwise processing and subcellular localization.* The EMBO journal, 2002. **21**(17): p. 4663-4670.
70. O'Brien, J., et al., *Overview of MicroRNA Biogenesis, Mechanisms of Actions, and Circulation.* Front Endocrinol (Lausanne), 2018. **9**: p. 402.
71. Ruby, J.G., C.H. Jan, and D.P. Bartel, *Intronic microRNA precursors that bypass Drosha processing.* Nature, 2007. **448**(7149): p. 83-86.
72. Xie, M., et al., *Mammalian 5'-capped microRNA precursors that generate a single microRNA.* Cell, 2013. **155**(7): p. 1568-1580.
73. Yang, J.-S., et al., *Conserved vertebrate mir-451 provides a platform for Dicer-independent, Ago2-mediated microRNA biogenesis.* Proceedings of the National Academy of Sciences, 2010. **107**(34): p. 15163-15168.
74. Gu, S. and M.A. Kay, *How do miRNAs mediate translational repression?* Silence, 2010. **1**(1): p. 11.
75. Park, J.H. and C. Shin, *MicroRNA-directed cleavage of targets: mechanism and experimental approaches.* BMB reports, 2014. **47**(8): p. 417.
76. Wu, L., J. Fan, and J.G. Belasco, *MicroRNAs direct rapid deadenylation of mRNA.* Proceedings of the National Academy of Sciences, 2006. **103**(11): p. 4034-4039.
77. Xu, W., et al., *Identifying microRNA targets in different gene regions.* BMC bioinformatics, 2014. **15**(S7): p. S4.
78. Dharap, A., et al., *MicroRNA miR-324-3p induces promoter-mediated expression of RelA gene.* PLoS one, 2013. **8**(11).

79. Paul, P., et al., *Interplay between miRNAs and human diseases.* Journal of cellular physiology, 2018. **233**(3): p. 2007-2018.
80. Smirnova, L., et al., *Regulation of miRNA expression during neural cell specification.* European Journal of Neuroscience, 2005. **21**(6): p. 1469-1477.
81. Li, Q.-J., et al., *miR-181a is an intrinsic modulator of T cell sensitivity and selection.* Cell, 2007. **129**(1): p. 147-161.
82. Calin, G.A., et al., *Frequent deletions and down-regulation of micro-RNA genes miR15 and miR16 at 13q14 in chronic lymphocytic leukemia.* Proceedings of the national academy of sciences, 2002. **99**(24): p. 15524-15529.
83. MacFarlane, L.-A. and P. R Murphy, *MicroRNA: biogenesis, function and role in cancer.* Current genomics, 2010. **11**(7): p. 537-561.
84. Di Leva, G. and C.M. Croce, *miRNA profiling of cancer.* Current opinion in genetics & development, 2013. **23**(1): p. 3-11.
85. Acunzo, M., et al., *MicroRNA and cancer–a brief overview.* Advances in biological regulation, 2015. **57**: p. 1-9.
86. Rosenfeld, N., et al., *MicroRNAs accurately identify cancer tissue origin.* Nature biotechnology, 2008. **26**(4): p. 462-469.
87. Schetter, A.J., et al., *MicroRNA expression profiles associated with prognosis and therapeutic outcome in colon adenocarcinoma.* Jama, 2008. **299**(4): p. 425-436.
88. Ma, J., C. Dong, and C. Ji, *MicroRNA and drug resistance.* Cancer gene therapy, 2010. **17**(8): p. 523-531.
89. Chen, H., et al., *Evaluation of plasma miR-21 and miR-152 as diagnostic biomarkers for common types of human cancers.* Journal of cancer, 2016. **7**(5): p. 490.
90. Benz, F., et al., *Circulating microRNAs as biomarkers for sepsis.* International journal of molecular sciences, 2016. **17**(1): p. 78.
91. Schwarzenbach, H., et al., *Clinical relevance of circulating cell-free microRNAs in cancer.* Nature reviews Clinical oncology, 2014. **11**(3): p. 145.
92. Si, H., et al., *Circulating microRNA-92a and microRNA-21 as novel minimally invasive biomarkers for primary breast cancer.* Journal of cancer research and clinical oncology, 2013. **139**(2): p. 223-229.
93. Matamala, N., et al., *Tumor microRNA expression profiling identifies circulating microRNAs for early breast cancer detection.* Clinical chemistry, 2015. **61**(8): p. 1098-1106.
94. Iorio, M.V., et al., *MicroRNA gene expression deregulation in human breast cancer.* Cancer Res, 2005. **65**(16): p. 7065-70.
95. Mattie, M.D., et al., *Optimized high-throughput microRNA expression profiling provides novel biomarker assessment of clinical prostate and breast cancer biopsies.* Mol Cancer, 2006. **5**: p. 24.
96. Blenkiron, C., et al., *MicroRNA expression profiling of human breast cancer identifies new markers of tumor subtype.* Genome Biol, 2007. **8**(10): p. R214.
97. Bhattacharyya, M., J. Nath, and S. Bandyopadhyay, *MicroRNA signatures highlight new breast cancer subtypes.* Gene, 2015. **556**(2): p. 192-8.
98. Li, L., et al., *Regulation of breast cancer tumorigenesis and metastasis by miRNAs.* Expert review of proteomics, 2012. **9**(6): p. 615-625.
99. Shen, F., et al., *MiR-492 contributes to cell proliferation and cell cycle of human breast cancer cells by suppressing SOX7 expression.* Tumor Biology, 2015. **36**(3): p. 1913-1921.

100. Lu, Y., et al., *MicroRNA-140-5p inhibits invasion and angiogenesis through targeting VEGF-A in breast cancer.* Cancer gene therapy, 2017. **24**(9): p. 386-392.
101. Sochor, M., et al., *Oncogenic microRNAs: miR-155, miR-19a, miR-181b, and miR-24 enable monitoring of early breast cancer in serum.* BMC cancer, 2014. **14**(1): p. 448.
102. Sun, Y., et al., *Serum microRNA-155 as a potential biomarker to track disease in breast cancer.* PloS one, 2012. **7**(10).
103. Zhou, X., et al., *MicroRNA-9 as potential biomarker for breast cancer local recurrence and tumor estrogen receptor status.* PloS one, 2012. **7**(6).
104. Jung, E.J., et al., *Plasma microRNA 210 levels correlate with sensitivity to trastuzumab and tumor presence in breast cancer patients.* Cancer, 2012. **118**(10): p. 2603-2614.
105. Nassar, F.J., et al., *miRNA as potential biomarkers of breast cancer in the Lebanese population and in young women: a pilot study.* PLoS One, 2014. **9**(9): p. e107566.
106. Nassar, F.J., et al., *microRNA Expression in Ethnic Specific Early Stage Breast Cancer: an Integration and Comparative Analysis.* Sci Rep, 2017. **7**(1): p. 16829.
107. Wang, S., et al., *The endothelial-specific microRNA miR-126 governs vascular integrity and angiogenesis.* Developmental cell, 2008. **15**(2): p. 261-271.
108. Meister, J. and M.H.H. Schmidt, *miR-126 and miR-126*: new players in cancer.* ScientificWorldJournal, 2010. **10**: p. 2090-100.
109. Ebrahimi, F., et al., *miR-126 in human cancers: clinical roles and current perspectives.* Exp Mol Pathol, 2014. **96**(1): p. 98-107.
110. Hua, Y., et al., *MicroRNA-126 inhibits proliferation and metastasis in prostate cancer via regulation of ADAM9.* Oncol Lett, 2018. **15**(6): p. 9051-9060.
111. Cammarata, G., et al., *Differential expression of specific microRNA and their targets in acute myeloid leukemia.* American journal of hematology, 2010. **85**(5): p. 331-339.
112. Ding, Q., et al., *MicroRNA-126 attenuates cell apoptosis by targeting TRAF7 in acute myeloid leukemia cells.* Biochemistry and Cell Biology, 2018. **96**(6): p. 840-846.
113. Wang, C.-Z., P. Yuan, and Y. Li, *MiR-126 regulated breast cancer cell invasion by targeting ADAM9.* International journal of clinical and experimental pathology, 2015. **8**(6): p. 6547.
114. Rouigari, M., et al., *Evaluation of the Expression Level and Hormone Receptor Association of miR-126 in Breast Cancer.* Indian J Clin Biochem, 2019. **34**(4): p. 451-457.
115. Liu, Y., et al., *Tumor tissue microRNA expression in association with triple-negative breast cancer outcomes.* Breast Cancer Res Treat, 2015. **152**(1): p. 183-191.
116. Volinia, S., et al., *Levels of miR-126 and miR-218 are elevated in ductal carcinoma in situ (DCIS) and inhibit malignant potential of DCIS derived cells.* Oncotarget, 2018. **9**(34): p. 23543.
117. Hafez, M.M., et al., *MicroRNAs and metastasis-related gene expression in Egyptian breast cancer patients.* Asian Pac J Cancer Prev, 2012. **13**(2): p. 591-8.
118. Tavazoie, S.F., et al., *Endogenous human microRNAs that suppress breast cancer metastasis.* Nature, 2008. **451**(7175): p. 147-52.
119. Zhu, N., et al., *Endothelial-specific intron-derived miR-126 is down-regulated in human breast cancer and targets both VEGFA and PIK3R2.* Mol Cell Biochem, 2011. **351**(1-2): p. 157-64.
120. Hong, Z., et al., *MicroRNA1263p inhibits the proliferation, migration, invasion, and angiogenesis of triplenegative breast cancer cells by targeting RGS3.* Oncol Rep, 2019. **42**(4): p. 1569-1579.

121. Zhang, J., et al., *The cell growth suppressor, mir-126, targets IRS-1.* Biochem Biophys Res Commun, 2008. **377**(1): p. 136-40.
122. Qu, Y., et al., *Evaluation of MCF10A as a Reliable Model for Normal Human Mammary Epithelial Cells.* PLoS One, 2015. **10**(7): p. e0131285.
123. Alhasan, L., *MiR-126 Modulates Angiogenesis in Breast Cancer by Targeting VEGF-A - mRNA.* Asian Pac J Cancer Prev, 2019. **20**(1): p. 193-197.
124. Turgut Cosan, D., C. Oner, and F. Mutlu Sahin, *Micro RNA-126 coordinates cell behavior and signaling cascades according to characteristics of breast cancer cells.* Bratisl Lek Listy, 2016. **117**(11): p. 639-647.
125. ZHANG, H., et al., *Aidi Injection () Alters the Expression Profiles of MicroRNAs in Human Breast Cancer Cells.* Journal of Traditional Chinese Medicine, 2011. **31**(1): p. 10-16.
126. Gurrapu, S., et al., *Sema4C/PlexinB2 signaling controls breast cancer cell growth, hormonal dependence and tumorigenic potential.* Cell Death Differ, 2018. **25**(7): p. 1259-1275.
127. Xiang, G. and Y. Cheng, *MiR-126-3p inhibits ovarian cancer proliferation and invasion via targeting PLXNB2.* Reprod Biol, 2018. **18**(3): p. 218-224.
128. El Ansari, R., et al., *The amino acid transporter SLC7A5 confers a poor prognosis in the highly proliferative breast cancer subtypes and is a key therapeutic target in luminal B tumours.* Breast Cancer Res, 2018. **20**(1): p. 21.
129. Miko, E., et al., *miR-126 inhibits proliferation of small cell lung cancer cells by targeting SLC7A5.* FEBS Lett, 2011. **585**(8): p. 1191-6.